

**CASE FILE  
COPY**

## **SECOND INTERIM REPORT**

### **DEVELOPMENT OF A SHORT LENGTH COMBUSTOR FOR A SUPERSONIC CRUISE TURBOFAN ENGINE USING A 90-DEGREE SECTOR OF A FULL ANNULUS**

**By  
T. R. Clements**

**PRATT & WHITNEY AIRCRAFT  
FLORIDA RESEARCH AND DEVELOPMENT CENTER**

**Prepared For  
NATIONAL AERONAUTICS AND SPACE ADMINISTRATION**

**NASA Lewis Research Center  
Contract NAS3-11159**

1. Report No. NASA CR-120908		2. Government Accession No.		3. Recipient's Catalog No.	
4. Title and Subtitle DEVELOPMENT OF A SHORT LENGTH COMBUSTOR FOR A SUPERSONIC CRUISE TURBOFAN ENGINE USING A 90-DEGREE SECTOR OF A FULL ANNULUS				5. Report Date April 1972	
				6. Performing Organization Code	
7. Author(s) T. R. Clements				8. Performing Organization Report No. PWA FR-4854	
9. Performing Organization Name and Address Pratt & Whitney Aircraft Florida Research and Development Center P.O. Box 2691 West Palm Beach, Florida				10. Work Unit No.	
				11. Contract or Grant No. NAS3-11159	
12. Sponsoring Agency Name and Address NASA-Lewis Research Center 21000 Brookpark Road Cleveland, Ohio				13. Type of Report and Period Covered Interim Report	
				14. Sponsoring Agency Code	
15. Supplementary Notes Project Manager, P. J. Perkins, Air Breathing Engine Procurement Section, NASA Lewis Research Center, Cleveland, Ohio					
16. Abstract  <p style="text-align: center;"><u>ABSTRACT</u></p> <p>An additional performance development program has been conducted on a short length, double-annular, ram-induction combustor. The combustor was designed for a large augmented turbofan engine capable of sustained flight speeds up to Mach 3.0. The outer liner diameter is 40 inches (1.01 m). The combustion length is 12 inches (0.305 m) from the fuel nozzle to the turbine inlet vane. The combined diffuser-combustor length is 20 inches (0.508 m). Performance tests were conducted at an inlet temperature and Mach number simulating engine sea level takeoff conditions. At the design temperature rise of 1600°F (889°K), combustion efficiency was 100%, pattern factor was 0.20, and combined diffuser-combustor pressure loss was 4.4% or 1.12 times the diffuser inlet velocity head. A temperature rise in excess of 2400°F (1333°K) with a combustion efficiency of 94% was demonstrated.</p>					
17. Key Words (Suggested by Author(s)) Combustor, Ram-Induction, Short Length, Double Annular, Performance				18. Distribution Statement  Unclassified - Unlimited	
19. Security Classif. (of this report) Unclassified		20. Security Classif. (of this page) Unclassified		22. Price* 3.00	
				21. No. of Pages 45	

\* For sale by the National Technical Information Service, Springfield, Virginia 22151

## FOREWORD

This interim report was prepared by the Pratt & Whitney Aircraft Division of United Aircraft Corporation under Contract NAS3-11159.

The contract was administered by the Air-Breathing Engine Procurement Section of the National Aeronautics and Space Administration, Lewis Research Center, Cleveland, Ohio.

The report summarizes the technical effort that was conducted during the period April 1970 through August 1971.

## CONTENTS

	PAGE
SUMMARY .....	1
INTRODUCTION .....	1
SCOPE OF THE INVESTIGATION .....	2
COMBUSTOR DESIGN .....	8
CALCULATIONS .....	13
RESULTS AND DISCUSSIONS .....	15
SUMMARY OF RESULTS .....	28
APPENDIXES .....	30
A - Equivalent Conical Angle .....	30
B - Test Facility and Test Rig Description .....	31
C - Instrumentation .....	33
REFERENCES .....	37

## ILLUSTRATIONS

FIGURE		PAGE
1	14-deg (0.244-rad) ECA Spreader-Type Diffuser, Initial Design .....	4
2	7-deg (0.122-rad) ECA Snout-Type Diffuser .....	5
3	9-deg (0.157-rad) ECA Dump Diffuser .....	6
4	Fuel Nozzle .....	7
5	Radial Inflow Fuel Nozzle Air Swirler .....	7
6	Ram Induction Concept in a Double-Annular Combustor .....	9
7	Single- and Double-Annulus Ram-Induction Combustors .....	10
8	Model 8, 256-Scoop Combustor (View Looking Upstream) ...	11
9	Flow Area Distribution (Percent); Model 8 and Model 9 Combustors .....	12
10	Model 9, 512-Scoop Combustor (View Looking Upstream) ...	12
11	Explanation of Terms in $\delta$ Rotor Expression .....	15
12	Outlet Radial Temperature Profile; Model 8 Combustor Installed in 7-deg (0.122-rad) ECA Diffuser .....	17

# ILLUSTRATIONS (Continued)

FIGURE		PAGE
13	Igniter Positions . . . . .	18
14	Ignition and Flameout Performance of the Model 8 Combustor . . . . .	18
15	Outlet Radial Temperature Profile; Model 8 Combustor Installed in 14-deg (0.244-rad) Diffuser . . . . .	19
16	Outlet Radial Temperature Profile; Model 9 Combustor in Initial Design 14-deg (0.244-rad) ECA Diffuser . . . . .	20
17	14-deg (0.244-rad) ECA Diffuser Instrumentation . . . . .	21
18	Shroud Hanger Bracket . . . . .	22
19	Capture Hoods . . . . .	22
20	Comparison of Initial and Final Design Flow Spreader for 14-deg (0.244-rad) ECA Diffuser . . . . .	23
21	Outlet Radial Temperature Profile; Model 9 Combustor Installed in Final Design 14-deg (0.244-rad) ECA Diffuser . . . . .	24
22	Outlet Radial Temperature Profile; Model 9 Combustor Installed in 9-deg (0.157-rad) Dump Diffuser . . . . .	25
23	Outlet Temperature Distribution; Model 9 Combustor Installed in 9-deg (0.157-rad) ECA Dump Diffuser . . . . .	26
24	Combustor Efficiency vs Fuel/Air Ratio; Model 8 Combustor . . . . .	27
25	Outlet Radial Temperature Profile; Model 8 Combustor Installed in 7-deg (0.122-rad) ECA Diffuser . . . . .	27
26	Double-Annular Combustor Test Rig . . . . .	31
27	Test Rig Installation, D-33B Test Stand . . . . .	32
28	Test Rig Cross Section Showing Instrumentation Planes . . . . .	34
29	5-Point Inlet Total Pressure Rake . . . . .	35
30	Outlet Total Temperature and Total Pressure Rake . . . . .	36

## TABLES

TABLE		PAGE
I	Combustor Performance Data for Double Annular Ram Induction Combustor . . . . .	16

## SUMMARY

An additional performance development program has been conducted on a short length combustor designed for a Mach 3.0, augmented, turbofan engine. The combustor is a double-annulus, ram-induction type, with an outer diameter of 40 inches (1.016 m) and a length of 12 inches (0.305 m) from fuel nozzle to turbine inlet vane. The combined diffuser-combustor length is 20 inches (0.508 m).

Testing was conducted in a full-scale, 90-deg (1.57-rad) sector rig. Test conditions were at a combustor inlet temperature, pressure, and Mach number of 600°F (589°K), 16 psia (11.03 N/cm<sup>2</sup>), and 0.244, respectively.

Previously reported development efforts provided a combustor configuration with good performance but with pressure loss higher than desirable (Reference 1). Efforts reported herein concentrated on reduction of pressure loss. An evaluation of the combustor performance at a temperature rise in excess of the 1600°F (889°K) design value was also conducted.

Two combustor and three diffuser configurations were investigated. Pressure loss was reduced from 5.6% to 4.4%. The combustion efficiency remained at 100% while the pattern factor increased from 0.14 to 0.20 at design conditions. A temperature rise capability in excess of 2400°F (1333°K) with a combustion efficiency of 94% was demonstrated.

## INTRODUCTION

The trend in combustion systems for modern high performance turbofan engines has been toward shorter length. Short length offers several advantages:

1. Cooling air requirements are reduced, making air available for combustion and outlet temperature pattern control.
2. Overall engine weight may be reduced.
3. Rotor lengths can be reduced, resulting in stiffer assemblies as well as reduced bearing requirements.

However, attaining a high level of performance in these systems can prove to be quite difficult.

Reducing the burning length generally results in decreased combustion efficiency as well as poor outlet temperature distributions. To overcome these problems, the turbulent mixing within the combustor must be increased, and the air distribution must be closely controlled to provide intimate mixing of the fuel and air. The double-annular, ram-induction concept reported herein provides a unique method of achieving these goals. The ram induction combustor differs from conventional combustors in that the ram pressure rather than the static pressure of the air is used to drive the flow into the combustor. Consequently less diffusion of the inlet air is needed with this design. The relatively high velocity air is captured by scoops in the combustor walls and turned into the combustion and dilution zones. Vanes are used in the scoops to reduce pressure loss caused by the high velocity turns. The high velocity and steep angle of the entering air jets promote rapid mixing of the fuel and air in the combustion zone and of the burned gases and air in the dilution zone. The

double-annular concept permits still further reduction of combustor length by maintaining an adequate ratio of effective combustor length to annulus height in the individual annuli as overall combustor length is shortened.

The potential of this concept to achieve good performance in an overall length of only 20 inches (0.508 m) was demonstrated under NASA Contract NAS3-7905 (Reference 2). Further development of the concept was undertaken under this contract, NAS3-11159, and, as reported in the first interim report (Reference 1), excellent results were obtained. The combustors described in Reference 1 yielded high efficiency (100%), low temperature pattern factors (0.14), and good radial temperature profiles. Similar results were obtained in full annular tests of this combustor conducted by the NASA as described in Reference 3. However, the pressure losses obtained were higher than desired. This report describes efforts to reduce the pressure loss of the system without seriously affecting the remaining performance parameters.

The test program was conducted at the Pratt & Whitney Aircraft Florida Research and Development Center in a full-scale sector rig that was a quarter section of a full annulus. All testing was performed at ambient pressure levels.

### SCOPE OF THE INVESTIGATION

The test program included the evaluation of two low pressure loss combustors and three diffuser configurations. The ignition and flameout capabilities of the combustors were determined and temperature rises in excess of 2400°F (1333°K) were demonstrated.

Combustors - The primary objective of the test program was to reduce the overall diffuser-combustor system total pressure loss without affecting the remaining performance parameters. The obvious first step was to simply increase the combustor air entry area. The two configurations studied in the initial phase of the program (Reference 1) that gave the best performance were increased in flow area from approximately 205 in<sup>2</sup> (1322.6 cm<sup>2</sup>) to 256 in<sup>2</sup> (1651.6 cm<sup>2</sup>). The combustors differed only in the number of air entry scoops. One configuration, designated Model 8, had 256 air entry scoops. The other, designated Model 9, had 512 scoops. In both combustors the air injection angle was 90-deg (1.57 rad) to the combustor centerline. The scoop pattern in both configurations was staggered as described in the section on combustor design. However, in the 512-scoop design, the pattern repeated twice per nozzle spacing and in the 256-scoop design, once per nozzle spacing.

Diffusers - The following three diffusers were used in the program:

1. A 14-deg (0.244-rad) equivalent conical angle (ECA), spreader-type diffuser. (ECA is defined in Appendix A.) A cross section of this diffuser is shown in figure 1. As shown, the spreader plates divided the inlet flow into three streams, one stream feeding each of the three combustor liners. The radial locations of the initial design spreader plates were such that the area splits at the spreader inlet matched the flow area splits of the combustor. The spreader was placed far enough downstream so that sufficient diffusion could be incorporated to reduce turning losses. Diffusion from the diffuser inlet to the spreader inlet was at an ECA of 14 deg (0.244 rad), giving an area ratio of 1.237. During the course

of the test program modifications, which are discussed later, were made to this design to provide more uniform airflow at the combustor.

2. A 7-deg (0.122 rad) ECA snout-type diffuser. A cross section of this diffuser is shown in figure 2. Contrasted with the 14-deg (0.244-rad) diffuser, the inner and outer walls of the flow spreader have been extended so as to become an integral part of the combustor. This provides a controlled path for the airflow feeding the inner and outer combustor liners. By eliminating the spreader blockage and the venting between the three diffuser streams (as occurs in the 14-deg (0.244-rad) diffusers), the dome pressure drop was increased. Diffusion occurs only in the initial portion of the diffuser; the area ratio was 1.245 from the diffuser inlet plane to the snout inlet.
3. A 9-deg (0.157-rad) ECA dump-type diffuser. A cross section of this diffuser is shown in figure 3. This design eliminates the problem of intermittent and spacially random flow separation by providing controlled separation at the diffuser exit. The four vane spreader at the exit was installed to aid in evenly spreading the flow over the combustor. An additional and important advantage is the mechanical simplicity of this diffuser compared with designs 1 and 2.

Fuel Injection - In all of the combustion tests the fuel was admitted to the combustion zone through simplex-type nozzles (figure 4). Two different flow ranges were utilized to cover the range of temperature rises investigated. The nozzles were fitted with a radial inflow swirler, shown in figure 5, which directed swirler air radially in toward the fuel nozzle centerline. After mixing with the fuel, the mixture was injected axially into the combustor through a 0.840-in. (0.021-m) diameter hole in the downstream face of the swirler. The minimum effective flow area of the swirler was 0.395 in<sup>2</sup> (2.55 cm<sup>2</sup>), based on flow data supplied by the NASA. The discharge coefficient was determined to be 0.50.

Measured Parameters - The test rig was instrumented to measure the following:

1. Combustor Airflow
2. Combustor Fuel Flow
3. Inlet Total and Static Pressure
4. Inlet Total Temperature
5. Outlet Total Temperature
6. Outlet Total Pressure (Outlet static pressure was assumed to be ambient.)

Instrumentation to measure diffuser static and total pressures at various locations were added as needed.



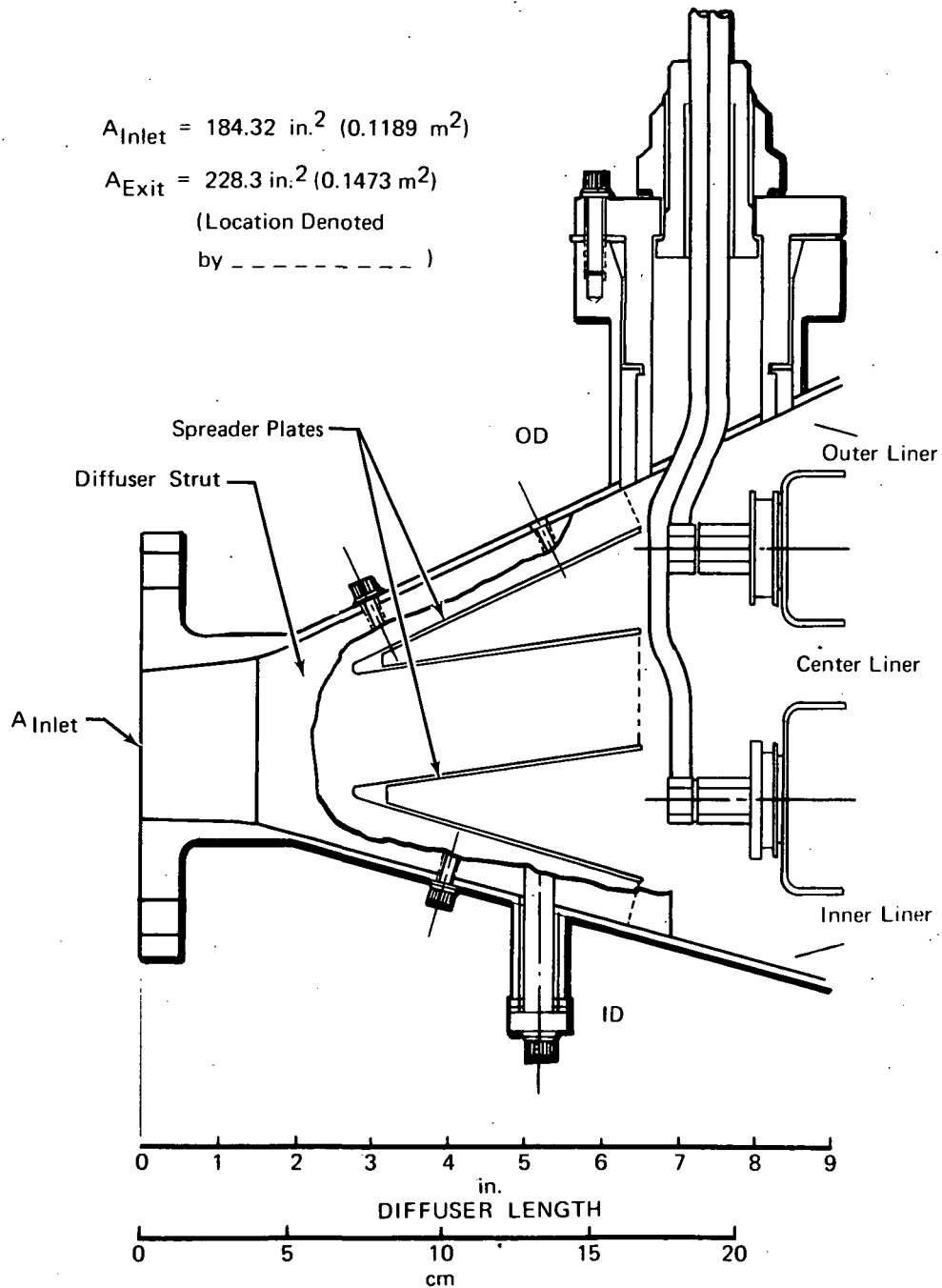


Figure 1. 14-deg (0.244-rad) ECA Spreader-Type Diffuser, Initial Design

FD 56938A

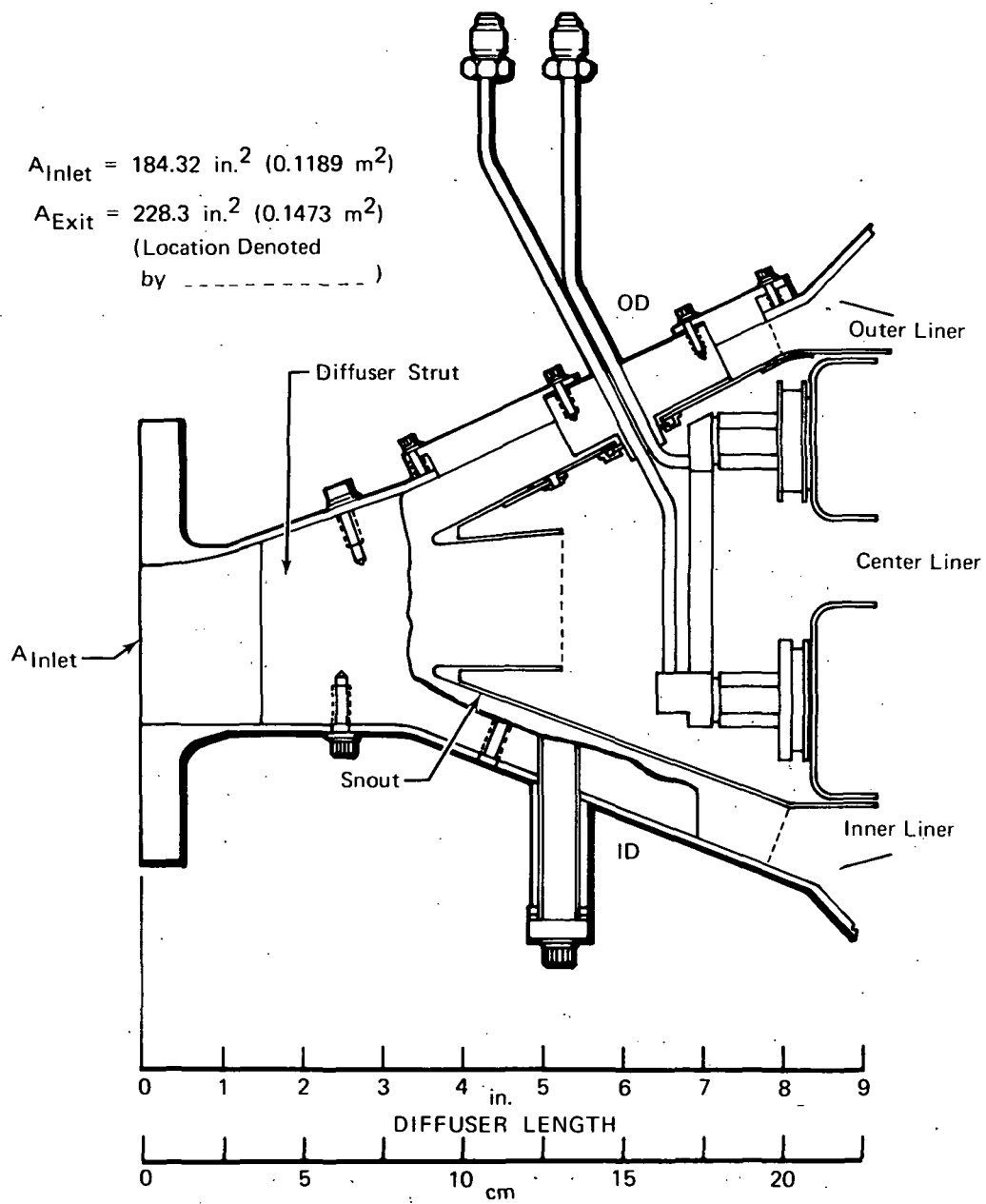


Figure 2. 7-deg (0.122-rad) ECA Snout-Type Diffuser

FD 56939A

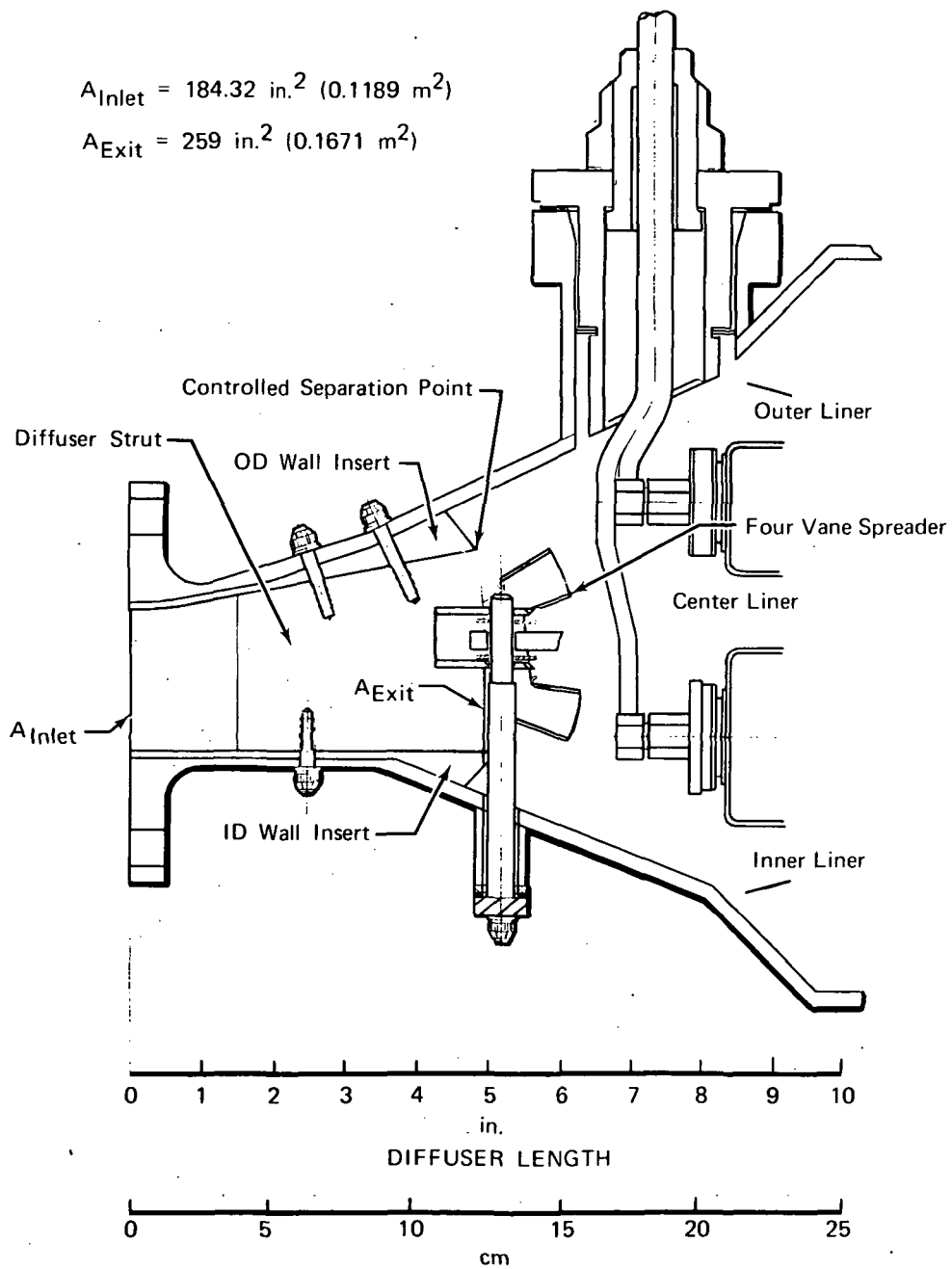


Figure 3. 9-deg (0.157-rad) ECA Dump Diffuser

FD 56940A

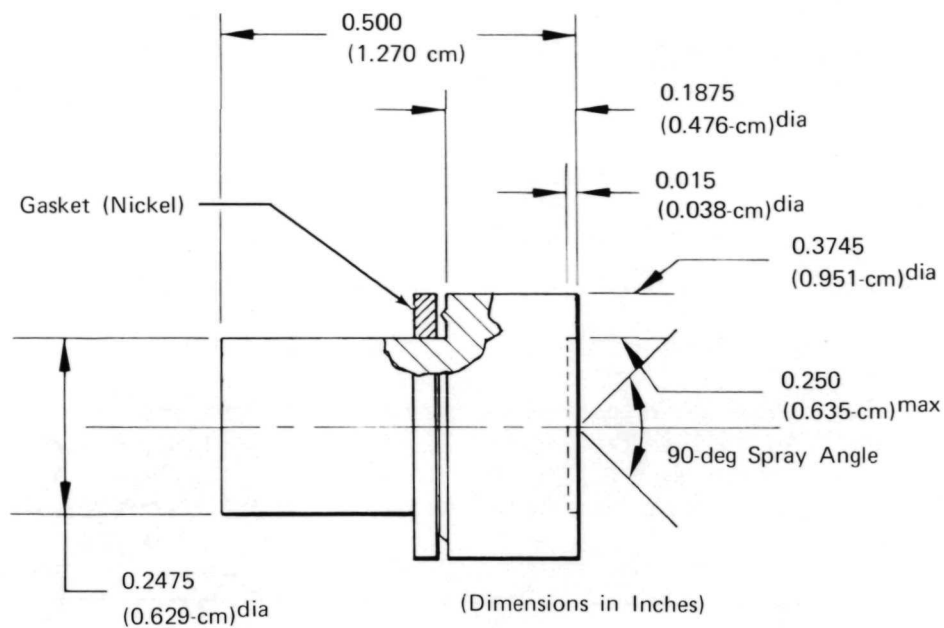


Figure 4. Fuel Nozzle

FD 36582A

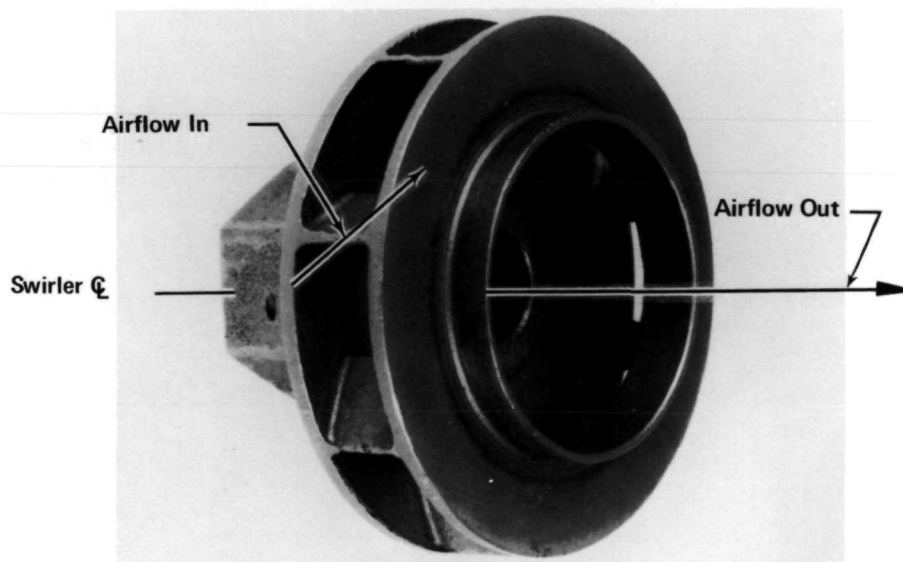


Figure 5. Radial Inflow Fuel Nozzle Air Swirler

FD 36586

Test Conditions - The test program was conducted at the nominal conditions listed below:

Inlet Total Pressure	- 16 psia (11.03 N/cm <sup>2</sup> )
Inlet Total Temperature	- 600 °F (588.7 °K)
Reference Velocity	- 100 ft/sec (30.4 m/s). This corresponds to an inlet Mach number of 0.244.
Average Outlet Temperature	- 2200 °F (1477.6 °K)

For a portion of those tests in which the temperature rise across the combustor was greater than the design  $\Delta T$  of 1600 °F (889 °K), the inlet temperature was reduced to 400 °F (478 °K). This was done to prevent damage to the outlet temperature probe. In all cases the nominal inlet Mach number of 0.244 was maintained.

The ignition tests were conducted at the following conditions:

Inlet Total Temperature	- 100 °F to 200 °F (311 °K to 367 °K)
Inlet Total Pressure	- 16 psia (11.03 N/cm <sup>2</sup> )
Reference Mach Number	- 0.038 to 0.075

#### COMBUSTOR DESIGN

Double-Annular, Ram-Induction Principle - The combustor used in this investigation is referred to as a double-annular, ram-induction combustor (sometimes called twin-ram induction combustor). The term "ram induction" arises because the air enters the combustor by the ram pressure of the inlet airflow. The airflow is efficiently turned into the combustion zone by several rows of vaned turning elbows or scoops, as shown in figure 6. This is contrasted with more conventional combustion systems where the airflow is first diffused to very low Mach numbers to increase the stream static pressure and is then forced to enter the combustor by the static pressure differential across the chamber walls.

Ram induction offers several advantages over conventional static pressure fed systems:

1. Better control of the airflow injection angle is obtained with the vaned turning scoops. This allows a shorter length combustor because more intense mixing can be established in the combustion zone.
2. Diffuser length can be shortened because diffusion to very low Mach numbers is no longer needed or desired. The overall diffuser-combustor length can therefore be reduced. The short length, small area ratio diffuser could have less pressure loss because it is not as prone to flow separation. However, this may be offset due to increased turning losses associated

with spreading the relatively high velocity flow evenly around the combustor.

3. The uniformity of the airflow supplied to the combustor is improved because a small area ratio diffuser with conservative equivalent conical angles (ECA) virtually eliminates diffuser stall.
4. The high velocity flow over the exterior surfaces of the combustor provides substantial convective cooling of these walls. This reduces the film cooling air requirement, making more air available for mixing and temperature profile control.

A more detailed discussion of the ram-induction concept is provided in Reference 4.

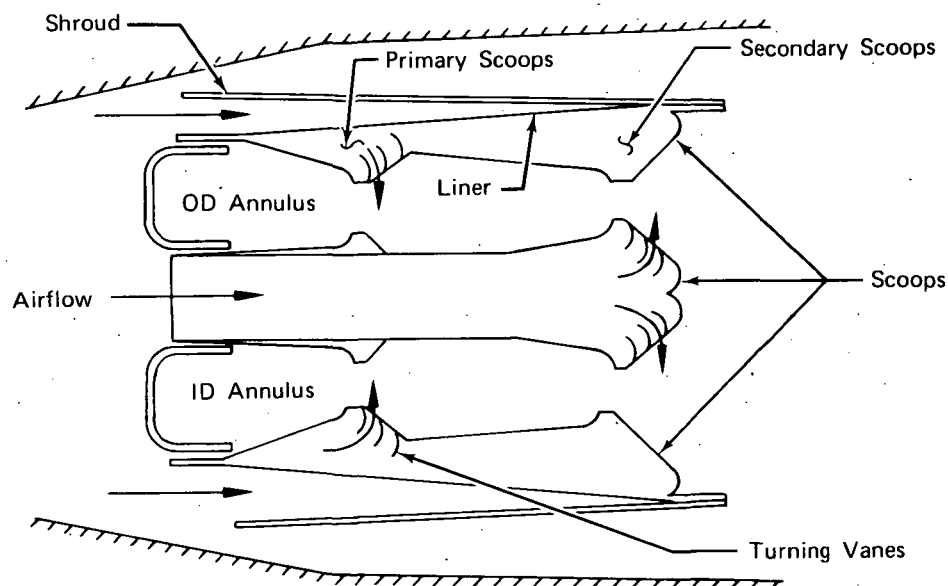


Figure 6. Ram Induction Concept in a Double-Annular Combustor

FD-36572A

Constructing the combustion zone as a double annulus allows a reduction in combustor length to be realized while maintaining an adequate ratio of effective combustor length to annulus height. This feature allows considerable reductions in combustor length to be made over that provided by use of the ram-induction concept alone. For example, figure 7 shows a comparison of a single-annulus, ram-induction combustor, tested by P&WA and the NASA (Reference 5), with the double-annular, ram-induction combustor. These combustor systems were designed to operate at similar conditions of Mach number, airflow, temperature, and pressure. The figures show that the combined diffuser-combustor length of the double-annular, ram-induction combustor is 10.2 inches (0.259 m) or 33% shorter.

Individual control of the inner and outer annulus fuel systems of the double-annular combustion zone provides a powerful method for tailoring the outlet radial temperature profile.

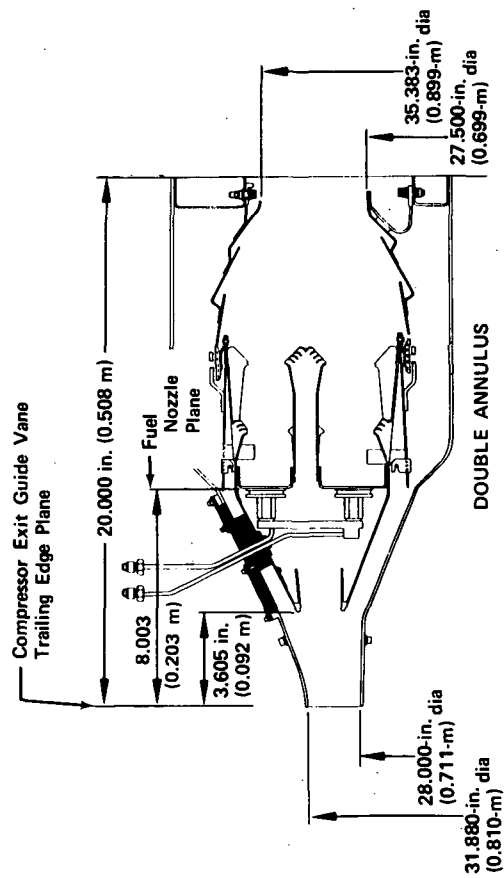
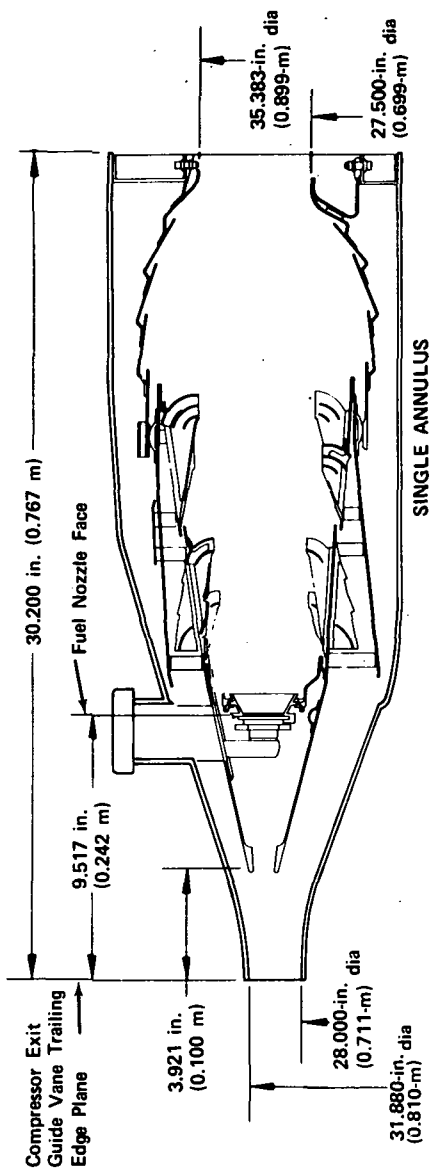


Figure 7. Single- and Double-Annulus Ram-Induction Combustors

FD 36584

Following is a brief description of the test combustors, both of which underwent minor modifications during the test program to correct deficiencies in performance.

Model 8 Combustor - This combustor (figure 8) consisted of 256 air entry scoops with 32 in the primary zone and 32 in the secondary zone for each liner air entry. The scoops were arranged so that the primary scoops on the outer and inner liners were in line with the fuel nozzle ports. The secondary scoops on these liners were then staggered relative to the primaries. The scoops on the center liner were staggered relative to their corresponding scoops on the OD and ID liners. Because there were 32 fuel nozzles in each combustion annulus, this pattern repeated once per nozzle spacing.

As stated above, the bulk of the liner cooling was accomplished by the high velocity flow over the exterior surfaces of the combustor. However, some localized film cooling was admitted through "thumb nail" scoops, as shown in figure 8. Film cooling air was also admitted through annular cooling gaps in the primary zone between the firewall and liners. Figure 9 gives the flow area distribution for the combustor.

Model 9 Combustor - This combustor, shown in figure 10, had 512 scoops with 64 scoops in the primary and 64 in the secondary for each liner. The staggered scoop arrangement used in the Model 8 was used in this design. However, because there were only 32 fuel nozzles, the scoop pattern repeated twice per nozzle spacing. The flow area distribution for this combustor was identical to the Model 8 combustor.

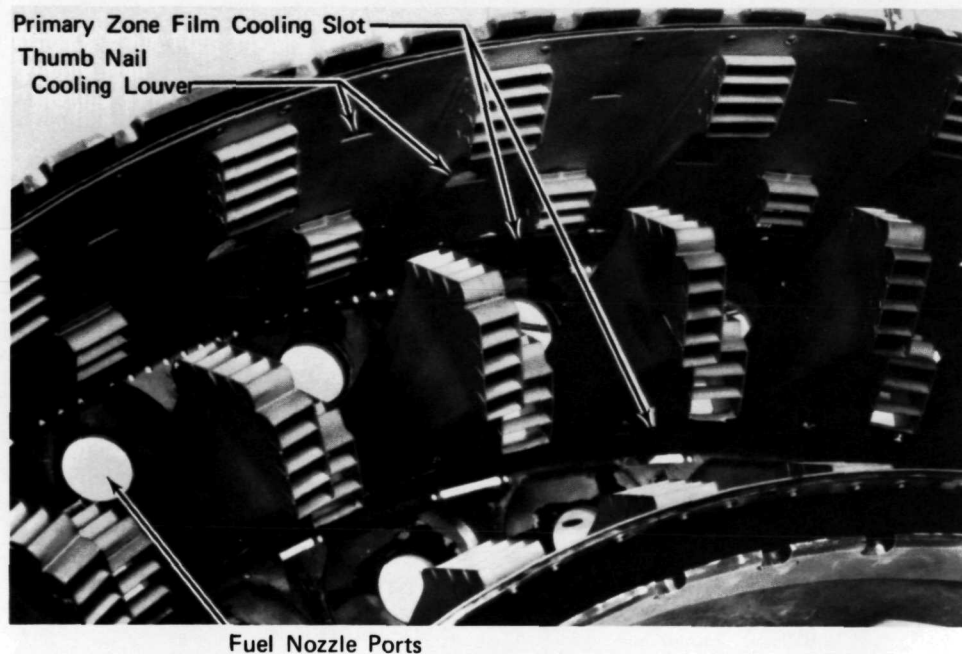


Figure 8. Model 8, 256-Scoop Combustor  
(View Looking Upstream)

FE 100226B



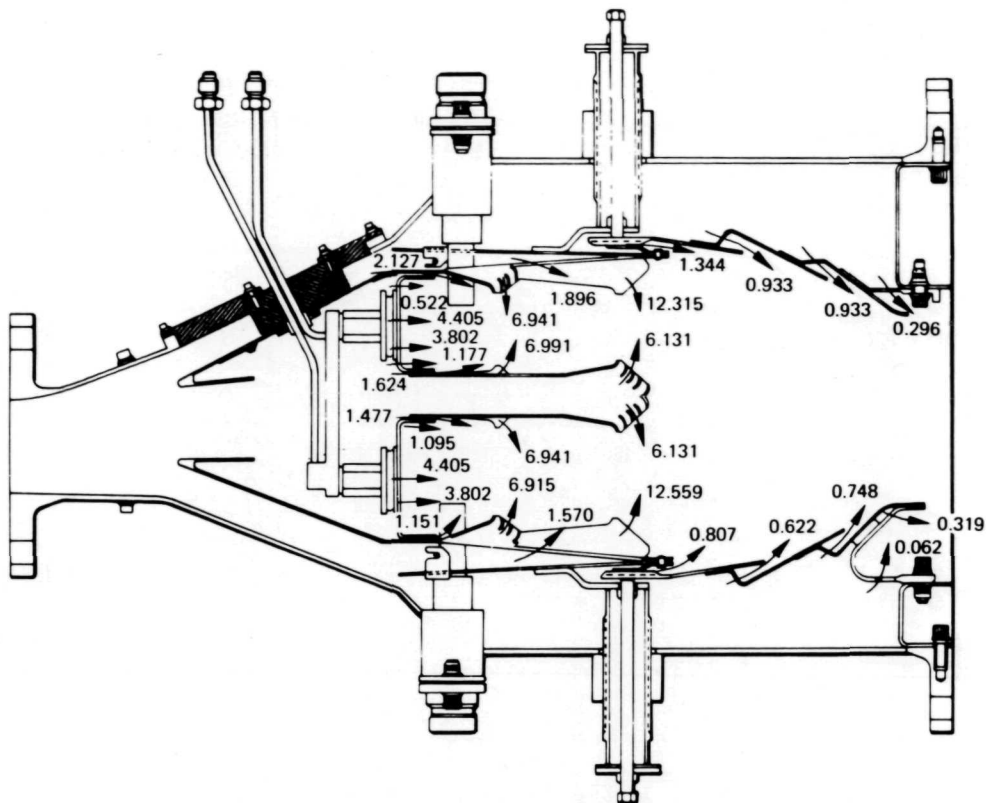


Figure 9. Flow Area Distribution (Percent);  
Model 8 and Model 9 Combustors

FD 31997A

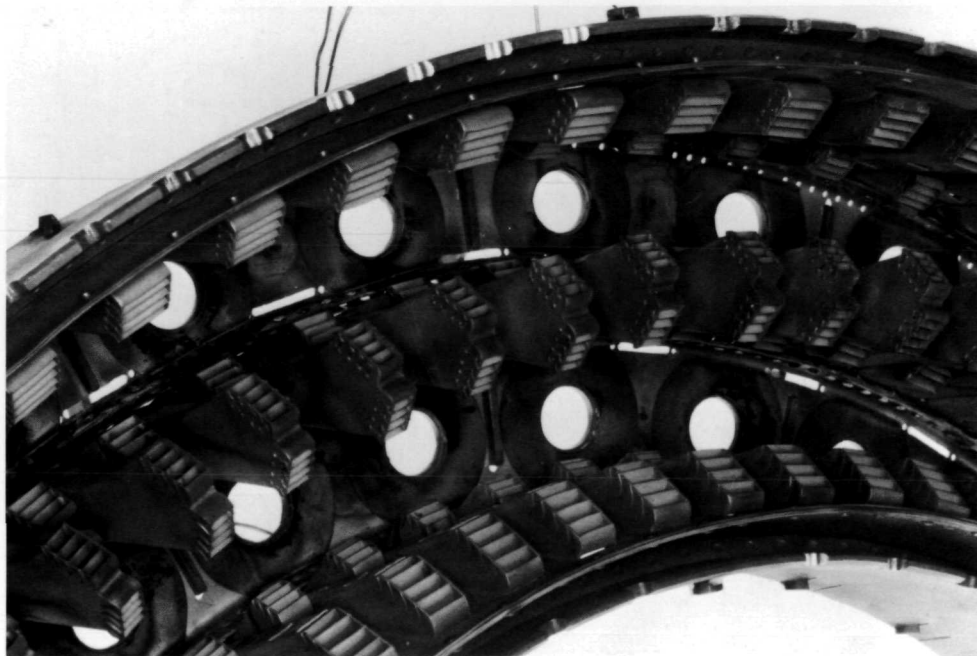


Figure 10. Model 9, 512-Scoop Combustor  
(View Looking Upstream)

FE 97605

## CALCULATIONS

Performance calculations included the determination of inlet Mach number, reference velocity, combustion efficiency, total pressure loss, and the outlet temperature uniformity parameters, TPF and  $\delta$  rotor.

Inlet Mach Number - Calculated from continuity using the average inlet static pressure and assuming one-dimensional isentropic flow. Therefore, the inlet Mach number is determined by

$$M_{n3} = \frac{W_{a3} \sqrt{T_{t3}}}{P_{s3} A_3} \sqrt{\frac{R}{\gamma \left[ 1 + \left( \frac{\gamma-1}{2} \right) M_{n3}^2 \right]}} \quad (\text{Eq 1})$$

where:

$M_n$  = Mach number

$W_a$  = Airflow

$T_t$  = Average total temperature of three readings

$P_s$  = Average static pressure of five readings

$A$  = Area

$\gamma$  = Ratio of specific heats

$R$  = Gas constant

The subscript 3 refers to the diffuser inlet plane.

Combustor Reference Velocity - Calculated assuming constant density flow from the diffuser inlet to the reference area. The reference area is defined as the inlet area between the inner and outer shrouds, which is approximately 711 in.<sup>2</sup> (0.428 m<sup>2</sup>). Therefore the reference velocity is determined by:

$$V_{\text{ref}} = \frac{W_{a3}}{\rho_3 A_s} \quad (\text{Eq 2})$$

where:

$V_{\text{ref}}$  = Reference velocity

$A_s$  = Shroud area

$\rho_3$  = Air density at diffuser inlet

Combustion Efficiency - Defined as the ratio of the measured temperature rise to a theoretical temperature rise. The theoretical rise is calculated from the

fuel-air ratio, fuel properties, inlet temperature, and the amount of water vapor present in the inlet airflow. The efficiency is expressed as:

$$\text{Eff}_{\text{mb}} = \frac{T_{t4m} - T_{t3}}{T_{t4w} - T_{t3}} \quad (\text{Eq 3})$$

where:

$\text{Eff}_{\text{mb}}$  = Combustion efficiency

$T_{t4m}$  = Mass weighted average of 105 outlet total temperatures

$T_{t4w}$  = Theoretical outlet total temperature

Total Pressure Loss - The combined diffuser-combustor total pressure loss is given by:

$$\frac{\Delta P}{P} = \frac{P_{t4} - P_{t3}}{P_{t3}} \quad (\text{Eq 4})$$

where:

$\frac{\Delta P}{P}$  = Total pressure loss expressed as a percentage of inlet total pressure

$P_{t3}$  = Mass weighted average of 25 inlet total pressures

$P_{t4}$  = Mass weighted average of 105 outlet total pressures

Outlet Temperature Pattern Factor (TPF) - Defined as the ratio of the maximum positive deviation from the average outlet temperature to the average temperature rise, or:

$$\text{TPF} = \frac{T_{t4 \text{ max}} - T_{t4}}{T_{t4} - T_{t3}} \quad (\text{Eq 5})$$

where:

TPF = Temperature pattern factor

$T_{t4 \text{ max}}$  = Maximum temperature at any location in the combustor outlet

Outlet Radial Temperature Profile - Determined from the average of 21 outlet total temperatures measured circumferentially at each of 5 radial positions.

$\delta$  Rotor - Defined as the ratio of the maximum positive deviation of the measured outlet radial temperature profile from a desired radial temperature profile to the desired temperature rise, or:

$$\delta \text{ rotor} = \frac{(T_{t4j} - T_{t4j \text{ desired}}) \text{ max}}{T_{t4 \text{ desired}} - T_{t3}} \quad (\text{Eq 6})$$

The "j" subscript refers to any radial location in the radial temperature profile. Note that the deviation is the maximum positive deviation at any radial location. Figure 11 is a graphical explanation of  $\delta_{\text{rotor}}$ . Because the desired profile is defined for some given outlet average temperature (in this case 2200° F (1477.6° K)), the measured profile must be normalized to that average temperature before comparison is made. This correction procedure is presented in Reference 1.

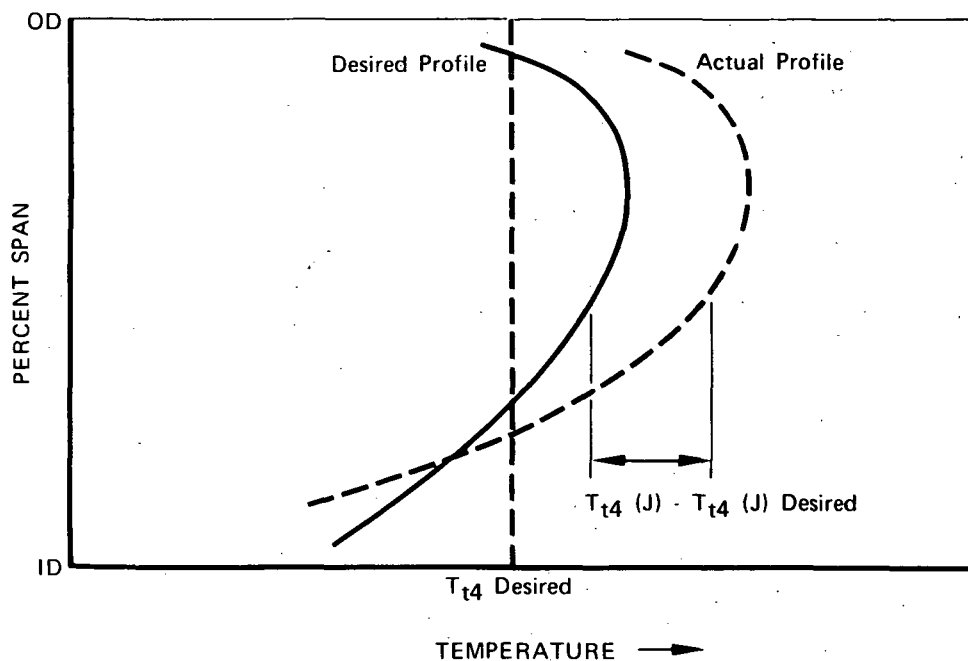


Figure 11. Explanation of Terms in  $\delta_{\text{Rotor}}$  Expression

FD 36573A

## RESULTS AND DISCUSSIONS

Model 8 - 256-Scoop Combustor - This combustor installed in the 7-deg (0.122 rad) snout-type diffuser demonstrated substantially superior performance compared with the Model 9, 512-scoop design discussed below. Table I summarizes the performance data for both designs. At the design temperature rise of 1600° F (889° K) combustion efficiency was 100%. The outlet temperature distribution was very uniform, as evidenced by the low temperature pattern factor of 0.20. The outlet radial temperature profile, as shown in figure 12, was an excellent approximation of the desired profile. The deviation,  $\delta_{\text{rotor}}$ , amounted to only 2.1% at the center of the profile. This profile was obtained using an equal fuel flow to each annulus or combustor zone.

The diffuser-combustor total pressure loss was decreased by 21%. In the high pressure loss version (as reported in Reference 1), the pressure loss was 5.6% at the design inlet Mach number of 0.244. The measured loss for this combustor was 4.4% or 112% of the inlet dynamic pressure. This value is within the state-of-the-art for current high performance engines.

Table I. Combustor Performance Data for Double Annular Ram Induction Combustor

Configuration			Combustor Inlet Conditions					Combustor Operating Conditions					Combustor Performance Characteristics							
Combustor	Diffuser	Remarks	Total Pressure psia	Total Pressure N/cm <sup>2</sup>	Temperature °F	Temperature °K	Airflow lb <sub>m</sub> /sec	Airflow kg/sec	Inlet Mach Number	Reference Velocity ft/sec	Fuel Air Ratio	OD/ID Fuel Split	Average Inlet Temperature °F	Average Inlet Temperature °K	Temperature Rise °F	Temperature Rise °K	Total Pressure Loss, %	Combustion Efficiency, %	Combustion Pattern Factor, TPF	δ Rotor*
Model 8 256 Scoop Combustor	7-degree (0.122 rad) ECA Shroud-Type Diffuser	Combustor had shroud capture hoods over OD and ID primary scoops.	15.7 10.8	610	584	4.98	2.21	2.33	0.244	97	29.6	0.024 1.0	2240 1500	1830 906	4.4	101	0.20	0.021		
			15.9 11.0	415	486	5.14	2.33	2.37	0.246	85	25.9	0.041 1.0	2786 1803	2371 1317	NA	96	0.15			
			15.8 10.9	404	480	5.22	2.37	2.33	0.238	85	25.9	0.043 1.0	2851 1839	2447 1359	NA	94	0.14			
			15.9 11.0	601	589	4.92	2.23	2.28	0.240	99	30.2	0.043 1.0	2927 1882	2326 92	NA	92	0.16			
Model 9 512 Scoop Combustor	14-degree (0.244 rad) ECA Diffuser	Combustor had shroud capture hoods over OD and ID primary scoops; diffuser was initial design with no modifications.	15.8 10.9	607	593	5.02	2.28	2.28	0.250	100	30.5	0.019 1.0	1931 1328	1324 786	4.6	101	0.27	0.075		
			15.7 10.8	588	582	4.99	2.28	2.25	0.247	98	29.9	0.025 0.908	2220 1489	1632 907	4.5	97	0.19	0.075		
			15.9 11.0	597	587	4.95	2.25	2.25	0.244	97	29.5	0.025 0.908	2182 1473	1595 886	4.5	96	0.21	0.029		
Model 9 512 Scoop Combustor	14-degree (0.244 rad) ECA Diffuser	Initial design combustor and diffuser.	15.7 10.8	588	582	5.01	2.27	2.27	0.248	98	29.9	0.020 1.0	1918 1321	1330 739	4.7	99	0.48			
	7-degree (0.122 rad) ECA Shroud-Type Diffuser	Initial design combustor.	No data taken due to aspiration of ID primary scoops																	
	14-degree (0.244 rad) ECA Diffuser	Initial design diffuser; combustor had shroud capture hoods over OD and ID primary scoops.	15.8 10.9	592	584	4.97	2.25	2.25	0.246	97	29.6	0.021 1.0	1884 1302	1292 718	4.6	94	0.39			
		Diffuser airflow splits matched to combustor flow area splits. Combustor had shroud capture hoods over OD and ID primary scoops.	16.9 11.7	616	598	5.19	2.35	2.35	0.242	97	29.6	0.023 1.0	2165 1458	1549 861	4.3	105	0.30	0.111		
	9-degree (0.157 rad) ECA Dump-Type Diffuser	Combustor had shroud capture hoods over OD and ID primary scoops.	15.9 11.0	610	594	4.97	2.25	2.25	0.244	98	29.9	0.024 1.0	2268 1516	1658 921	4.9	99	0.30	0.101		

NA - Not Available

\* - δ Rotor is defined for a specified desired radial profile at a specified average temperature (2200° F in this program). The average temperature of the measured radial profile must be corrected to the desired average temperature before δ rotor is determined. Since the correction procedure distorts the profile, δ rotor is not calculated for those profiles where the measured average temperature deviates from the design 2200° F (1478° K) temperature by more than 200° F (111° K).

NA - Not Available

\* - δ Rotor is defined for a specified desired radial profile at a specified average temperature (2200° F in this program). The average temperature of the measured radial profile must be corrected to the desired average temperature before δ rotor is determined. Since the correction procedure distorts the profile, δ rotor is not calculated for those profiles where the measured average temperature deviates from the design 2200° F (1478° K) temperature by more than 200° F (111° K).

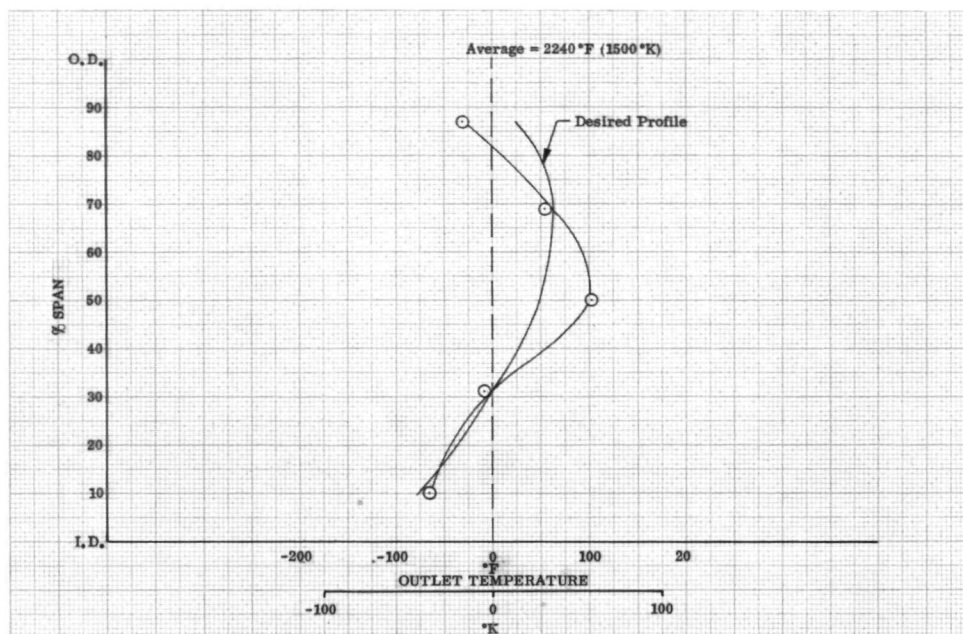


Figure 12. Outlet Radial Temperature Profile;  
Model 8 Combustor Installed in 7-deg  
(0.122-rad) ECA Diffuser

DF 88196

Lean ignition and flameout limits were measured at combustor inlet conditions simulating those occurring in an engine during standard day ground start ignition. The igniters were located as shown in figure 13. The data are summarized in figure 14. As the figure shows, the minimum ignition fuel-air ratio (0.008) occurred at the maximum reference Mach number (0.075). Flameout occurred at a constant 0.007 f/a regardless of test conditions.

The combustor was also tested with the 14-deg (0.244-rad) ECA diffuser. Performance was not as good as with the 7-deg (0.122-rad) ECA snout-type diffuser. With equal fuel flows in both combustion zones, the combustion efficiency was 100% within the limits of measurement accuracy. However, the temperature pattern factor was 0.27 compared to the 0.20 value obtained with the snout-type diffuser. The outlet radial temperature profile, figure 15, was a poor approximation of the desired profile. An improvement in pattern factor was obtained by adjusting the fuel flow into each annulus. With a 0.906 OD-to-ID annulus fuel flow ratio, the pattern factor dropped to 0.21. However, the combustion efficiency dropped to 96%. The outlet radial temperature profile, also shown in figure 15, was almost flat.

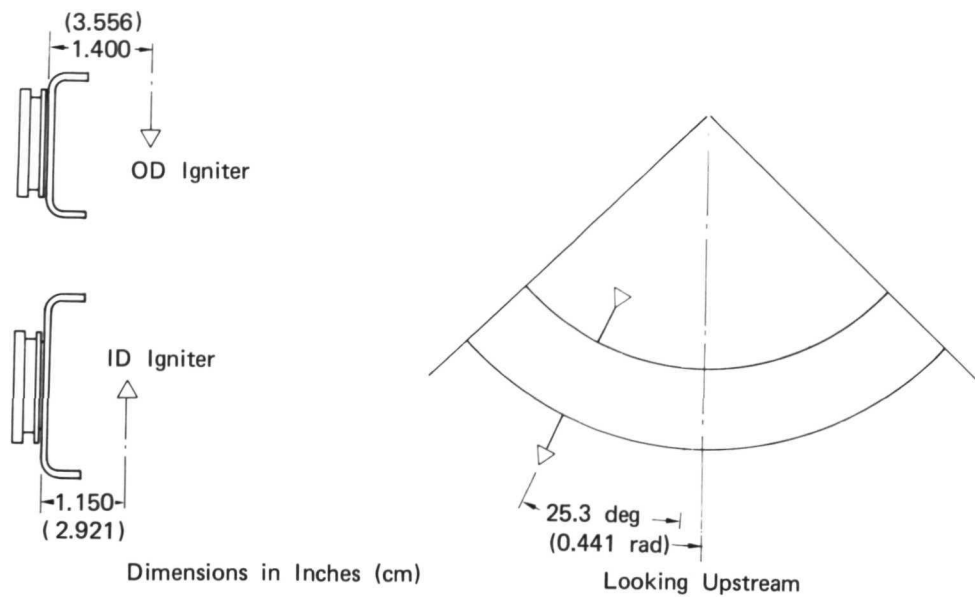


Figure 13. Igniter Positions

FD 39107B

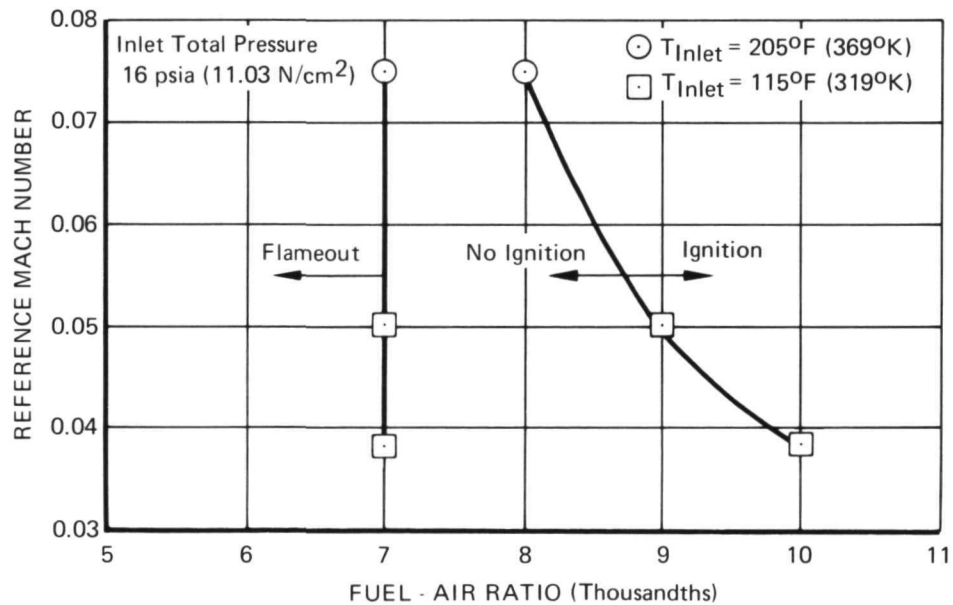


Figure 14. Ignition and Flameout Performance of the Model 8 Combustor

FD 59710

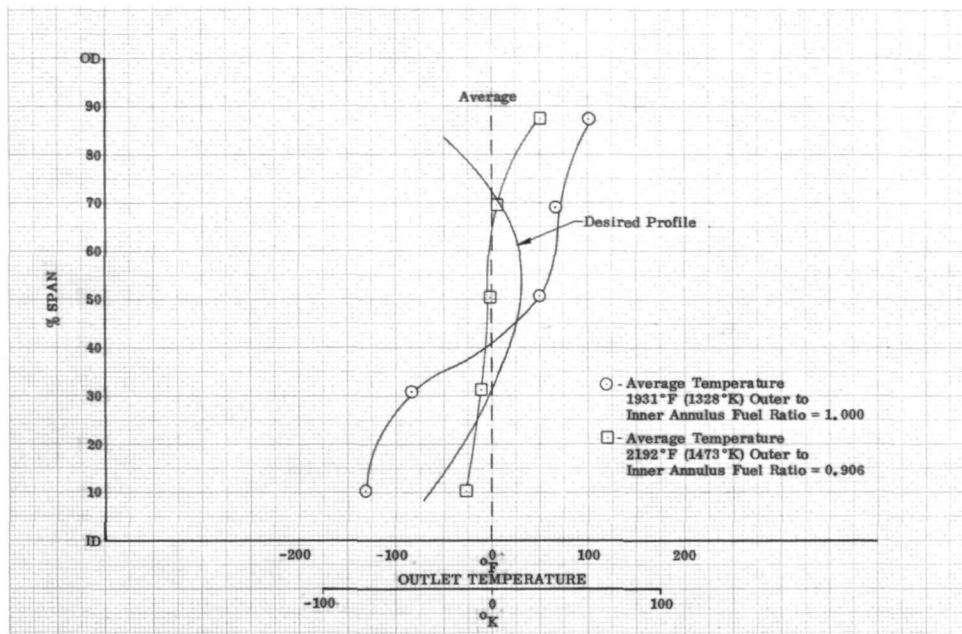


Figure 15. Outlet Radial Temperature Profile;  
Model 8 Combustor Installed in 14-deg  
(0.244-rad) Diffuser

DF 88199

Model 9 - 512-Scoop Combustor - This combustor did not perform very well. The primary problem was a lack of penetration from the OD and ID liner secondary scoops and overpenetration from the center secondary scoops. This was evidenced by the extremely center peaked outlet radial temperature profiles obtained. An extensive effort was undertaken to eliminate this situation. Several combustor and diffuser modifications were tested. Most of the diffuser development was done with the 14-deg (0.244-rad) ECA diffuser. When initially tested with the 14-deg (0.244-rad) diffuser, the temperature pattern factor was 0.48. The outlet radial temperature profile (figure 16) was extremely center peaked. The profile alone accounted for approximately 42% of the pattern factor. The combustion efficiency was 99%. The diffuser-combustor total pressure loss was unchanged from the Model 8, namely 4.4% at an inlet Mach number of 0.244. The combustor was then tested with the 7-deg (0.122-rad) ECA snout-type diffuser. Because of the low pressure loss of the combustor and the high shroud velocity associated with the ram-induction design, a reverse static pressure gradient across the inner liner primary scoops was created. This reverse gradient or aspiration caused hot combustion gases to be drawn through the scoops into the inner shroud, resulting in severe overheating of the inner liner and scoops. Some cold flow diagnostic tests were then performed to aid in correcting the aspiration problem. A pressure survey of the scoop discharges was made to determine the relative airflow distribution of the combustor. The 14-deg (0.244-rad) ECA diffuser was instrumented, as shown in figure 17, to obtain static pressure rise data and total pressure profiles at the inlet and outlet of the diffuser flow spreader. From these data relative airflow splits in the diffuser could be calculated. The data revealed (1) low air-flow through the primary scoops, (2) circumferential nonuniformity in primary



scoop airflow due to blockage by the shroud hangar brackets, figure 18, which were located in front of every other primary scoop, (3) a severe mismatch between the diffuser flow splits and combustor area splits, and (4) excessive diffuser dump losses. To correct these difficulties several modifications were made: (1) the hangar brackets were removed and shroud capture hoods, figure 19, were installed; shroud support was provided by the capture hoods, (2) the radial location of the diffuser flow spreader was altered to bring the diffuser airflow splits in line with the combustor area splits, and (3) the contour of the spreader walls was slightly altered to provide additional diffusion before dumping occurred. A comparison of the original flow spreader and the final design spreader is shown in figure 20. Performance improved; the outlet temperature pattern factor dropped from 0.48 to 0.30. However, approximately 48% of the pattern factor was accounted for in the very center peaked radial temperature profile (figure 21). The combustion efficiency remained high; measured efficiency was 105%. The overall total pressure loss was 4.3%.

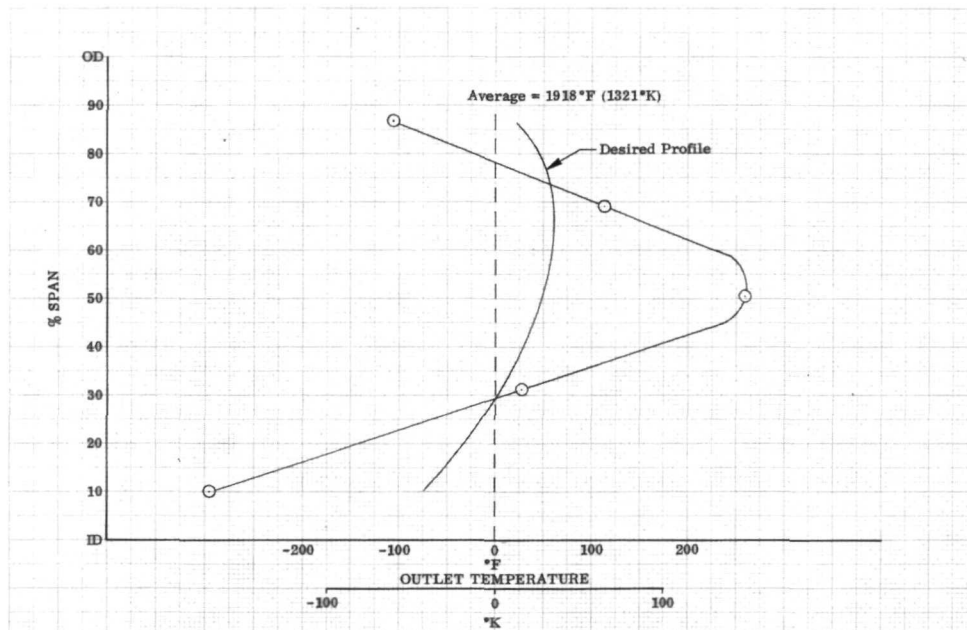


Figure 16. Outlet Radial Temperature Profile;  
Model 9 Combustor in Initial Design  
14-deg (0.244-rad) ECA Diffuser

DF 88201

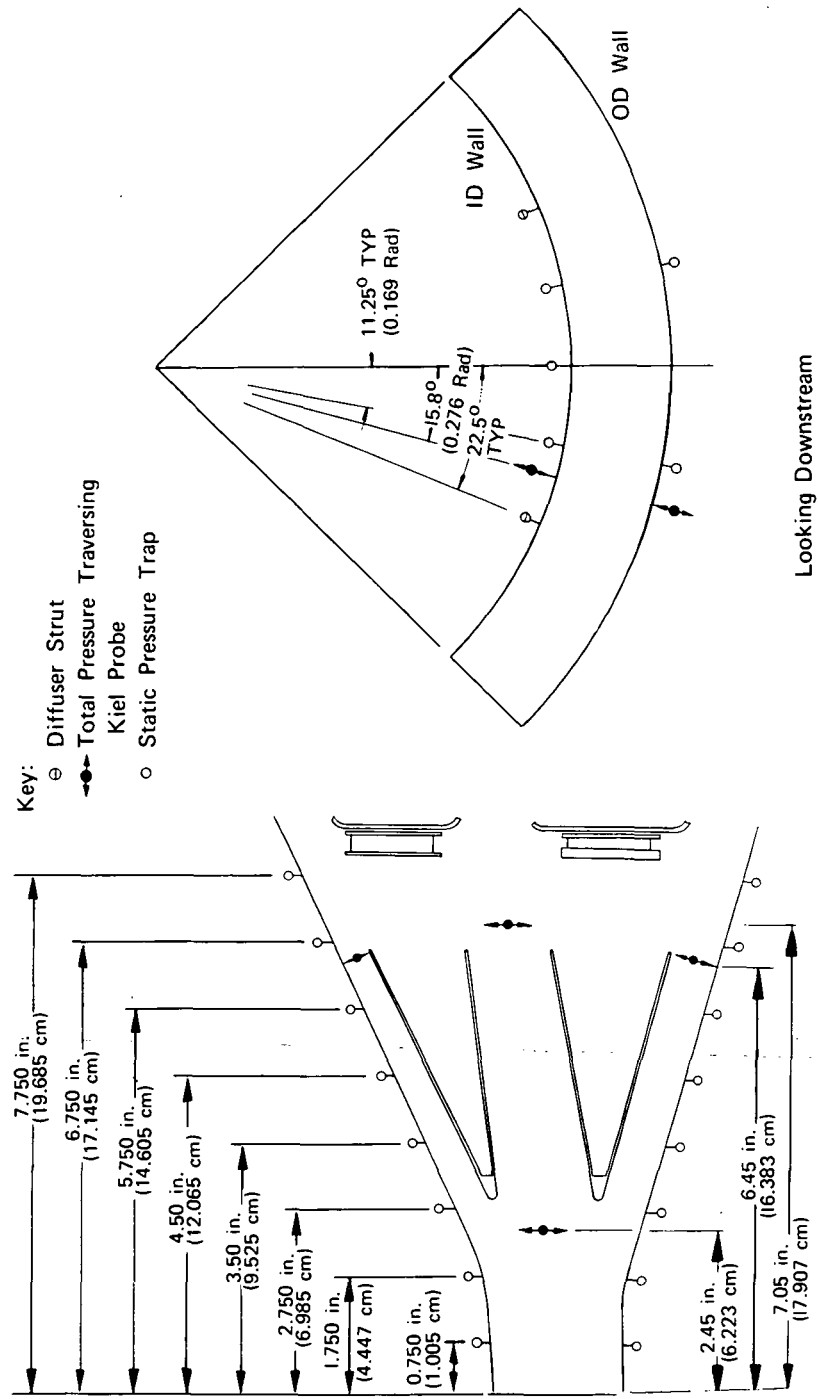


Figure 17. 14-deg (0.244-rad) ECA Diffuser Instrumentation

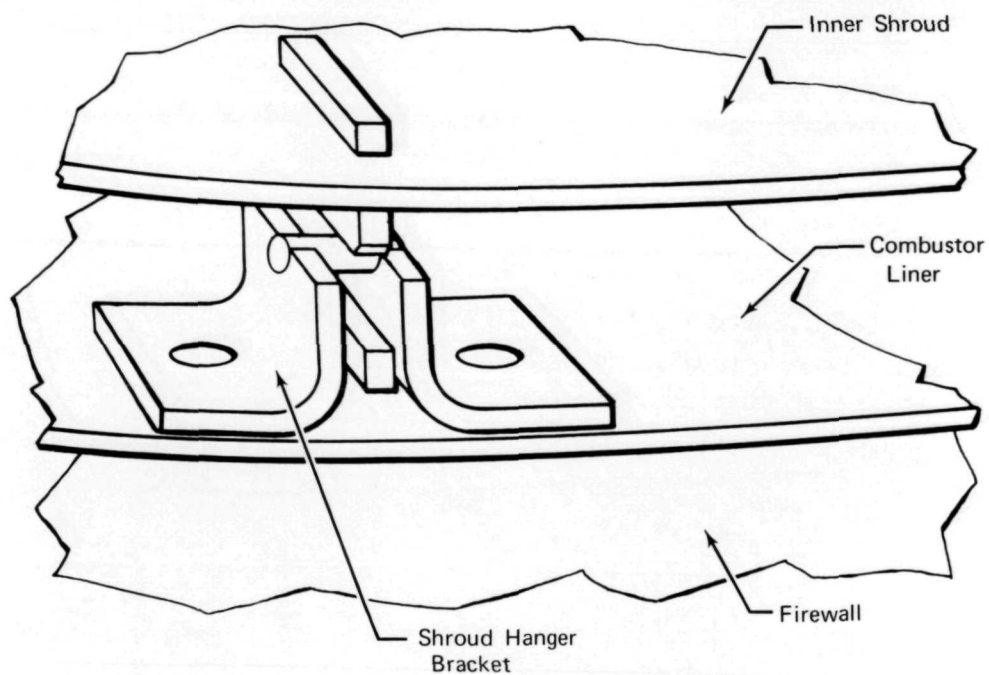


Figure 18. Shroud Hanger Bracket

FD 56941A

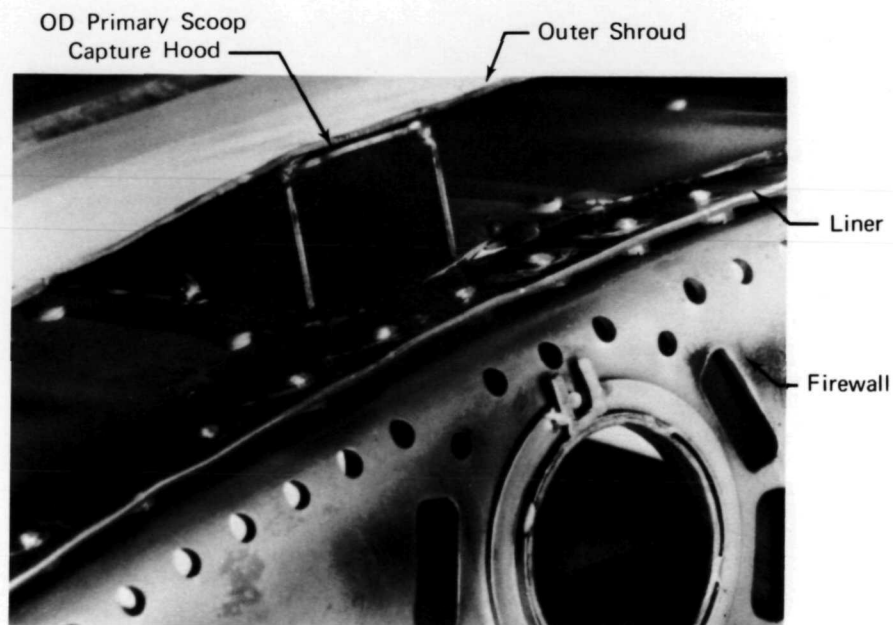


Figure 19. Capture Hoods

FE 100223B

Spreader Flow Areas  
In.<sup>2</sup> (cm<sup>2</sup>)

Design	Location	Inlet	Exit
Initial	O.D.	54.1 (349)	54.1 (349) 23.7%
	Center	121.7 (785)	121.7 (785) 53.3%
	I.D.	52.5 (339)	52.5 (339) 23.0%
	Total	228.3 (1473)	228.3 (1473)
Final	O.D.	81.9 (528)	95.0 (613) 36.5%
	Center	74.9 (483)	86.9 (561) 33.4%
	I.D.	67.4 (435)	78.2 (505) 30.1%
	Total	224.2 (1446)	260.1 (1679)

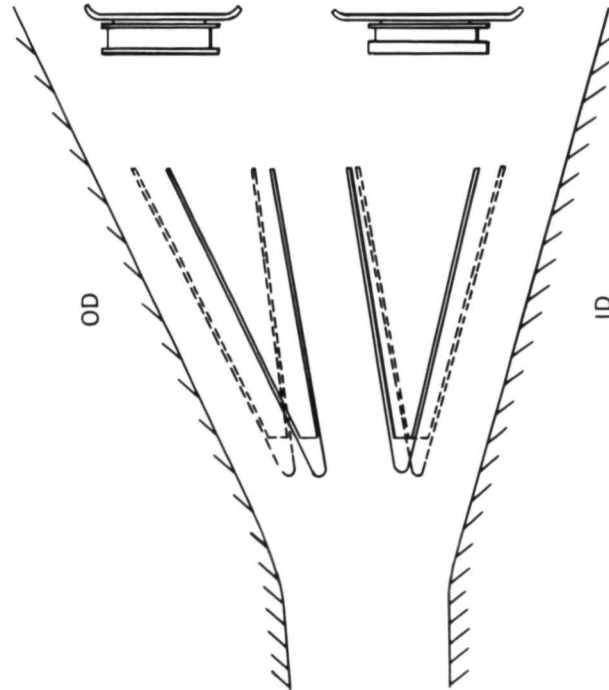


Figure 20. Comparison of Initial and Final Design Flow Spreader for 14-deg (0.244-rad) ECA Diffuser FD 56943

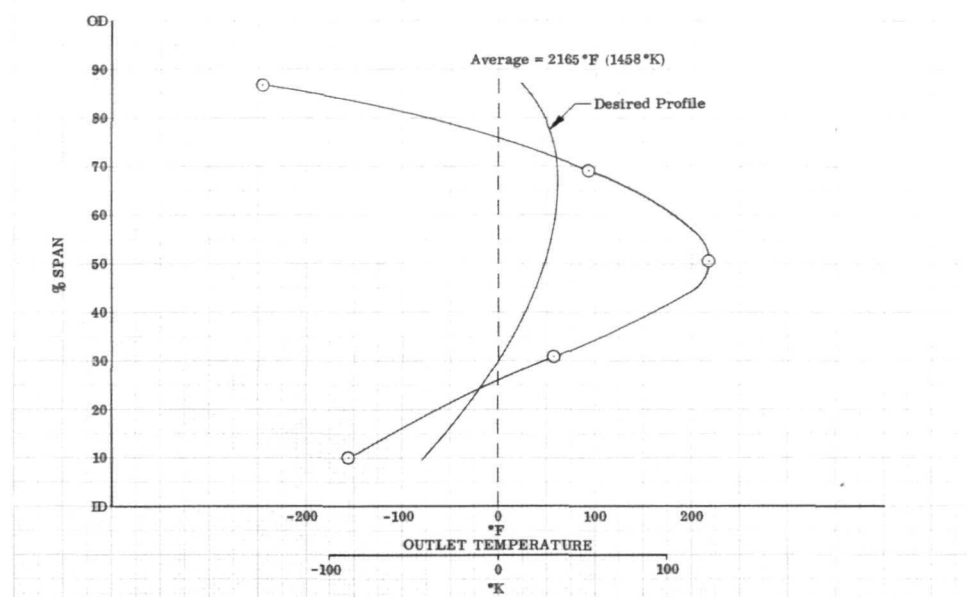


Figure 21. Outlet Radial Temperature Profile; DF 88202  
Model 9 Combustor Installed in Final  
Design 14-deg (0.244-rad) ECA  
Diffuser

Concurrently with the effort described above another diffuser concept was tested. This is the controlled separation or dump diffuser (figure 3) which is finding favor in many current engines. By diffusing at conservative rates and then providing controlled separation into a dump region, the uniformity of the airflow supplied to the combustor is generally very good. The dump diffuser has been used primarily in static pressure fed systems because the low diffuser exit Mach numbers required prevent excessive dump losses. With ram induction the exit Mach numbers are higher; consequently, the dump losses are higher. However, the benefits to be gained from a more uniform combustor inlet airflow as well as a more simplified mechanical design made the diffuser worthwhile for evaluation in the test program. With this diffuser, the Model 9 combustor demonstrated performance comparable with that obtained with the 14-deg (0.244-rad) diffuser. The total pressure loss did increase, rising to 4.9% from 4.4%. Combustion efficiency was 99% and the temperature pattern factor remained unchanged at 0.30. The outlet radial temperature profile (figure 22), as before, is extremely center peaked, accounting for 43% of the pattern factor. Although the performance was not improved over that obtained with the 14-deg (0.244-rad) case, the potential to do so is apparent in the overall temperature distribution (figure 23). This figure shows a very uniform distribution with a radial stratification of the isotherms. The high temperature region behind the left-hand (lower in the figure) diffuser strut was most likely the result of local flow separation from the strut. Disregarding that region and calculating the pattern factor for the remainder of the distribution yields a value of 0.19. A slightly more conservative diffusion angle should eliminate the possibility of any separation from the struts.

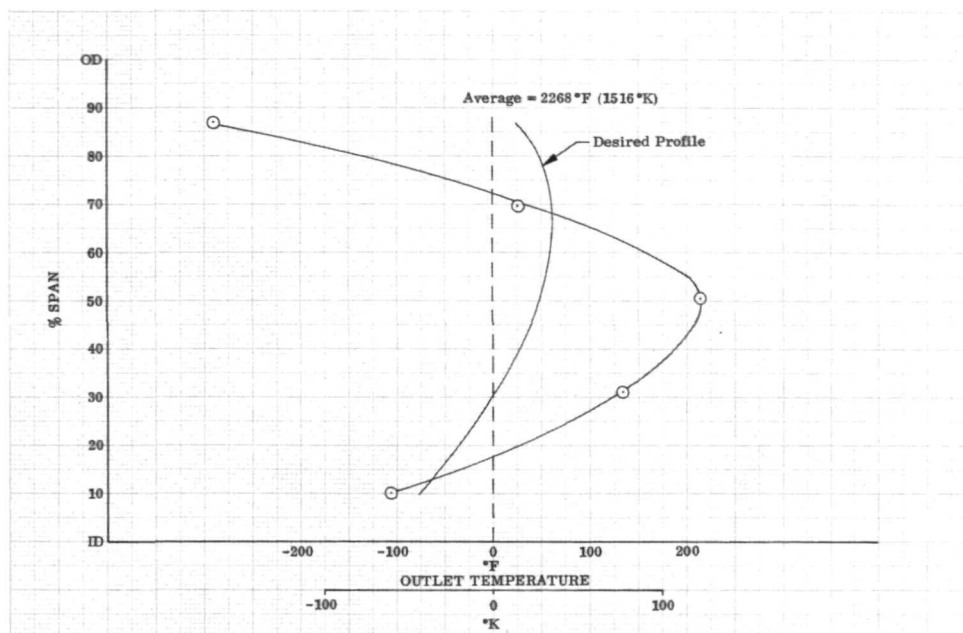


Figure 22. Outlet Radial Temperature Profile; DF 88203  
Model 9 Combustor Installed in 9-deg  
(0.157-rad) Dump Diffuser

High Temperature Rise Performance of the Model 8 Combustor - The Model 8 combustor was tested at fuel-air ratios up to 0.043. Except as noted the inlet temperature was 400°F (478°K). At the maximum fuel-air ratio the temperature rise was 2447°F (1359°K) giving an outlet temperature of 2847°F (1837°K). This corresponds to a combustion efficiency of 94%. As figure 24 shows, the combustion efficiency remained high over the entire range of fuel-air ratios investigated. The uniformity of the outlet temperature distribution as defined by the pattern factor improved with increasing fuel-air ratios dropping to a low of 0.014 at the maximum  $\Delta T$ . The decrease in pattern factor with increasing  $f/a$ , at high  $f/a$ , is not unexpected. As the fuel concentration approaches stoichiometric, the maximum temperature becomes fixed at the stoichiometric value. Therefore, as the average temperature rises, the pattern factor must decrease. The outlet radial temperature profile obtained at the maximum fuel-air ratio and 400°F (478°K) inlet temperature condition is shown in figure 25.

Pressure loss data for these high temperature rise tests were not available because the exit traverse probe used for these tests was not equipped with total pressure sensors. However, at a temperature rise of 2175°F (1208°K), for which pressure data were available, the measured loss was unchanged from the value obtained at lower temperature rises.

Approximately 8.75 hours of run time at outlet temperature levels in excess of 2400°F (1589°K) were accumulated with no physical damage to the combustor. In fact, no damage to the combustor was observed when the outlet temperature was increased to 2927°F (1882°K) with an inlet temperature of 600°F (589°K).

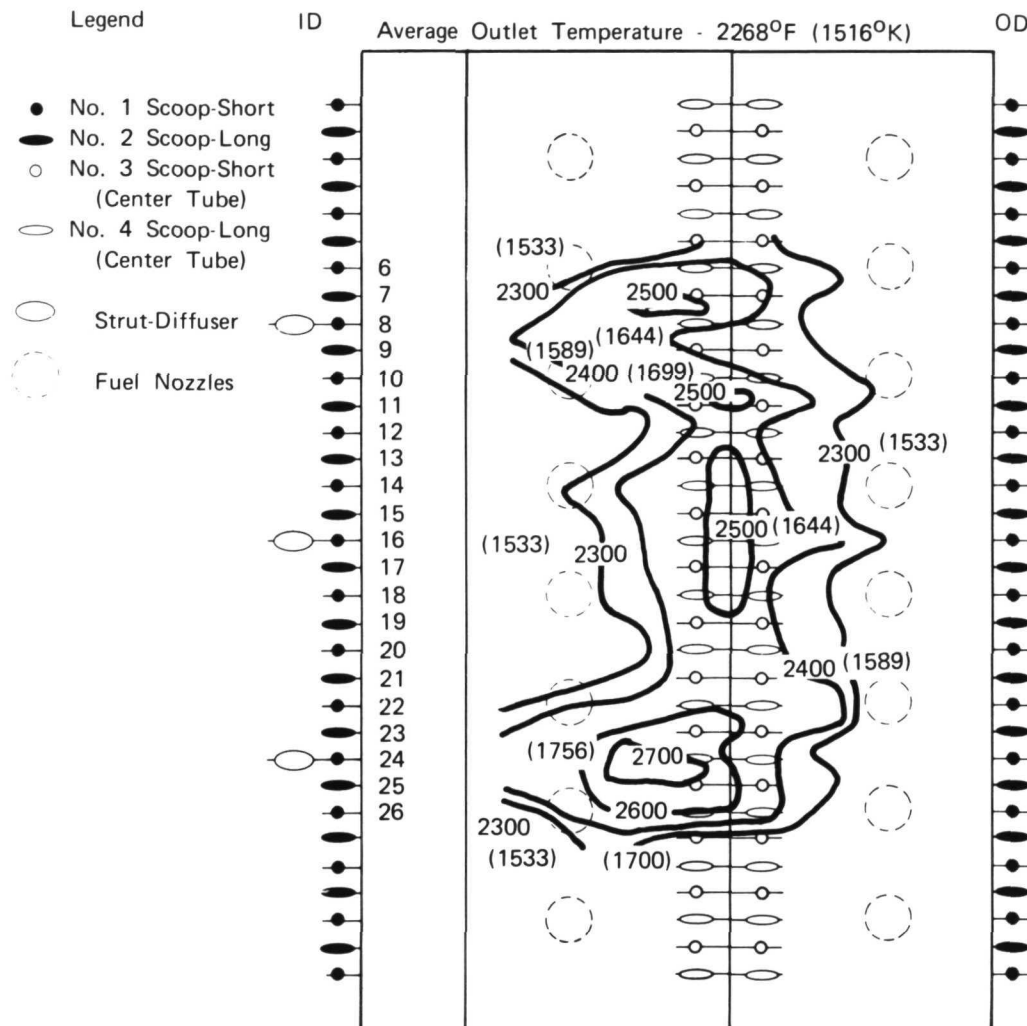


Figure 23. Outlet Temperature Distribution;  
Model 9 Combustor Installed in 9-deg  
(0.157-rad) ECA Dump Diffuser

FD 56944

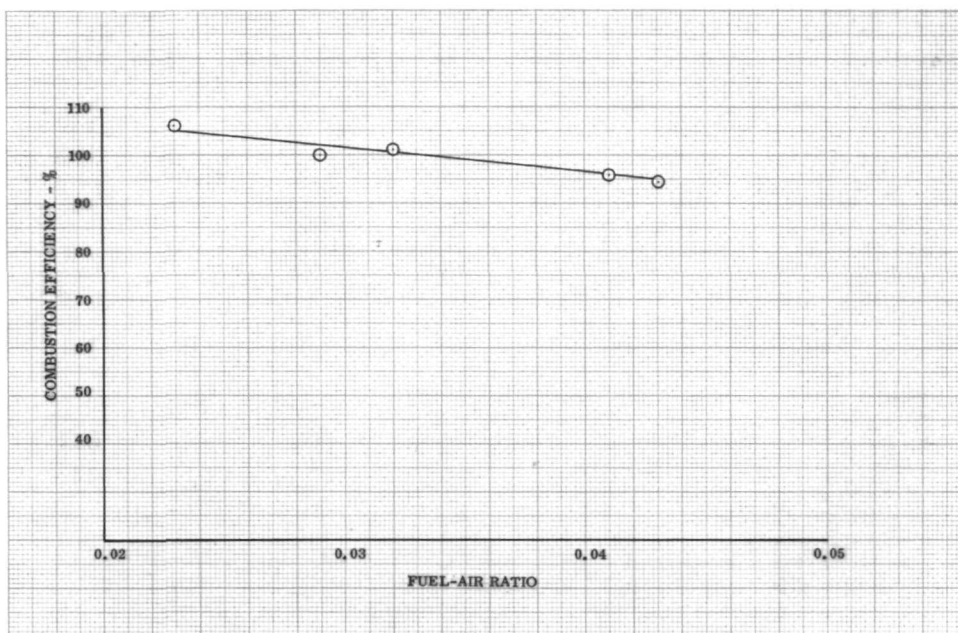


Figure 24. Combustor Efficiency vs Fuel/Air Ratio; Model 8 Combustor

DF 88197

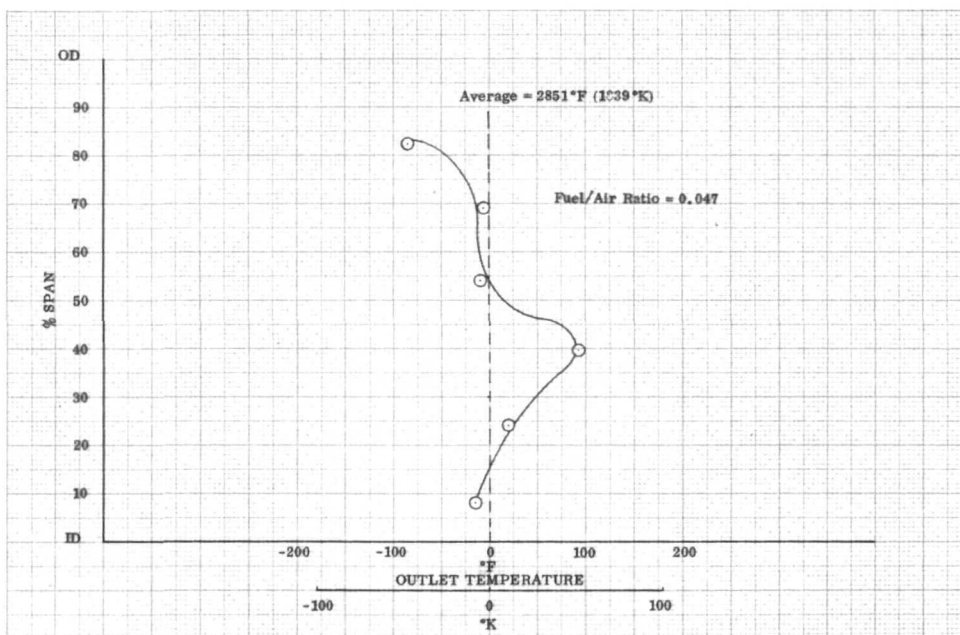


Figure 25. Outlet Radial Temperature Profile; Model 8 Combustor Installed in 7-deg (0.122-rad) ECA Diffuser

DF 88198



## SUMMARY OF RESULTS

An additional performance development program has been conducted on a double-annular ram-induction combustor to reduce the total pressure loss of an earlier design and to demonstrate a high temperature rise capability. Testing was accomplished in a sector rig, which was a quarter section of a full annulus. The test condition of 600°F (589°K) inlet air temperature and 100 ft/sec (30.48 m/sec) reference velocity simulated the sea level takeoff conditions of a high flight speed augmented turbofan engine. All testing was conducted at ambient pressure levels. The following results were obtained.

1. The 256-scoop combustor (Model 8) demonstrated the best performance. When tested with the 7-deg (0.122-rad) ECA diffuser the following results were obtained:
  - a. Total pressure loss was reduced to 4.4% compared to 5.6% in the earlier design. The diffuser inlet Mach number was 0.244. This lower value is within the state-of-the-art for current high performance engines.
  - b. Combustion efficiency was approximately 100% at the design temperature rise of 1600°F (889°K).
  - c. The combustor demonstrated a temperature rise capability of 2447°F (1359 °K) with a combustion efficiency of 94%. With an inlet temperature of 400°F (478 °K) the outlet temperature was 2847°F (1837 °K).
  - d. No physical damage to the combustor was noted after 8.75 hours of testing at outlet temperature levels between 2400°F (1333°K) and 2927°F (1882°K).
  - e. The radial temperature profile was a good approximation of the desired profile. The deviation,  $\delta$  Rotor, amounted to 2.1% at the midspan. This profile was obtained with an equal fuel flow to each annulus.
  - f. Temperature pattern factor was 0.20.
  - g. The combustor ignited at fuel/air ratios of approximately 0.009 at inlet temperatures and reference velocities simulating standard day ground start ignition. At these same conditions flameout occurred at a fuel/air ratio of 0.007.
2. The 512-scoop combustor (Model 9) suffered from a lack of penetration from the inner and outer liner secondary scoops and overpenetration from the center liner secondaries. As a result of this, all versions of this combustor produced severely center peaked exit temperature profiles.

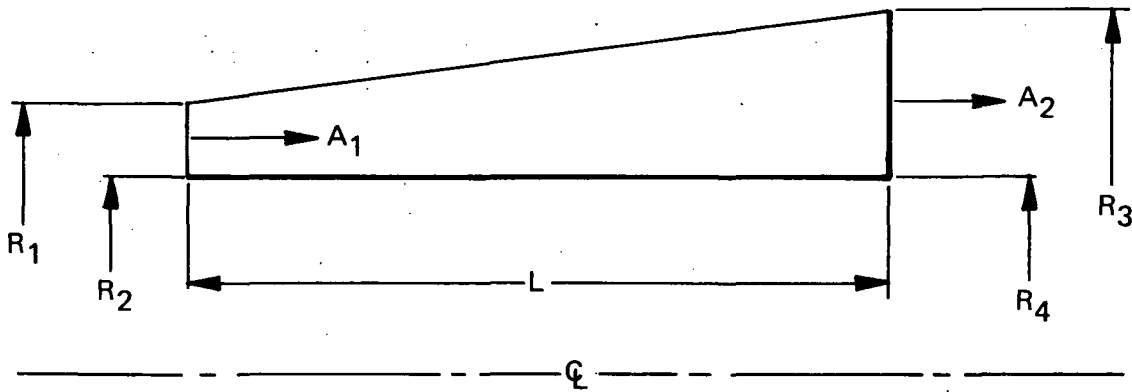
3. The aerodynamic studies conducted on the Model 9 combustor in the 14-deg (0.244-rad) ECA diffuser had the following results:
  - a. As the total pressure loss was reduced, capture hoods over the inner and outer liner primary scoops became essential to prevent aspiration.
  - b. Matching of the diffuser and combustor flow area splits was found to be unsatisfactory. Experimental matching of the diffuser airflow splits with the combustor flow area splits was necessary to obtain a more uniform airflow at the combustor.
4. The dump diffuser demonstrated the potential of achieving good performance due to the uniformity of the airflow supplied to the combustor. Although the measured pressure loss was high, careful interfacing of the diffuser and combustor should eliminate this problem. Except for the higher pressure loss, the performance of this simplified design was comparable with the 14-deg (0.244 rad) ECA diffuser.

## APPENDIX A - EQUIVALENT CONICAL ANGLE

**Definition** - The equivalent conical angle (ECA) is defined as the included angle of a conical diffuser that has the same area ratio, inlet area, and wetted surface area as the diffuser under investigation. For annular diffusers, ECA may be approximated by the following equation:

$$ECA = 2 \tan^{-1} \left[ \frac{\left( \frac{A_2}{A_1} - 1 \right) A_1}{\pi L (R_1 + R_2 + R_3 + R_4)} \right]$$

Where the symbols are defined by:



**Application** - The above equation for ECA does not consider the presence of struts in the diffusing passage. The equation was used only to arrive at an area ratio for a given ECA and diffusing length assuming that no struts were in the passage. In adding struts, the diffuser wall exit radii were adjusted to maintain the same area ratio.

## APPENDIX B - TEST FACILITY AND TEST RIG DESCRIPTION

Test Facility - All combustion tests were conducted on test stand D-33B at the P&WA Florida Research and Development Center. Combustion air was supplied by bleeding the compressor discharge of a JT4 turbojet engine. Airflow rate was controlled by a pneumatically operated 10-inch (25.4-cm) inlet butterfly valve with vernier control by a 4-inch (10.16-cm) pneumatically operated supply line bleed valve.

The test stand fuel system was capable of supplying each of three combustion zones with 300 pph (136.08 kg/hr) of ASTM-A1 type fuel at 750-psig (517-N/cm<sup>2</sup>) fuel pressure. Control room monitoring of fuel pressure and temperature was provided for each zone.

The test facility had high pressure steam service available to operate steam ejectors. The ejectors were needed to aspirate the outlet temperature traverse probe.

Test Rig Description - A brief description of the major components of the combustor test rig is presented below. For reference, a cross section of the rig is presented in figure 26 and the rig installation in the D-33B test facility in figure 27. The rig was constructed entirely of AISI type 347 stainless steel.

Flow Straightener - This section was designed to smooth out any irregularities in rig inlet airflow and to provide a near stagnation region for accurate measurement of inlet total pressure and temperature. The flow straightener was fabricated from a 12-inch (30.480-cm) diameter cylinder 24 inches (60.960 cm) long. A bank of 1.5-inch (3.81-cm) diameter tubes 12 inches (30.480 cm) long was used to straighten the inlet airflow.

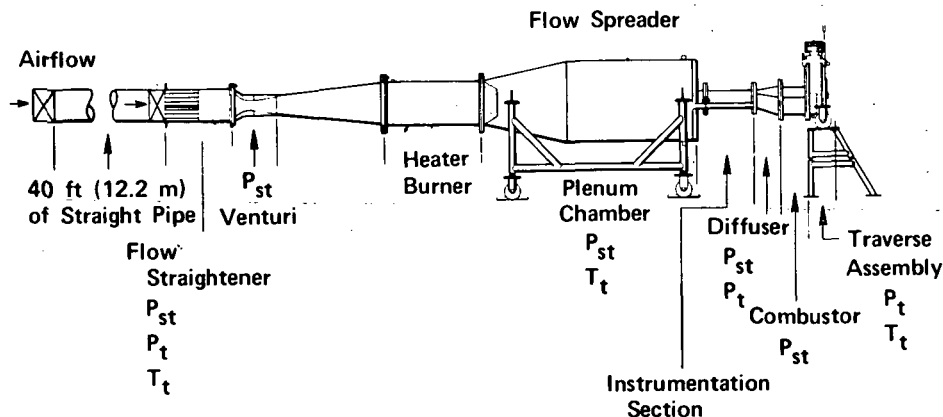
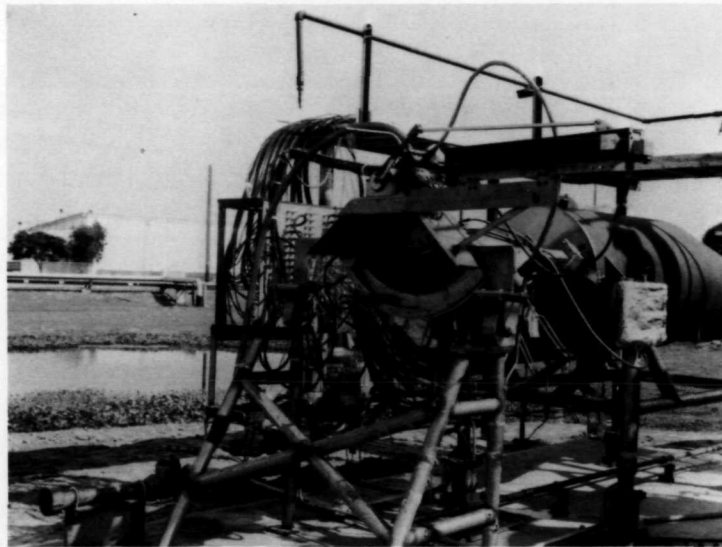


Figure 26. Double-Annular Combustor Test Rig

FD 13874C

Venturi - This section provided accurate airflow measurement with minimum pressure loss. The rig airflow entered through a constant radius inlet to a 4.7483-inch (12.0607-cm) diameter throat. Transition from the venturi throat to the preheater inlet was provided by a conical diffusing section 40.840 inches (103.7 cm) long with a 12-deg, 31-min (0.218-rad) included angle.



FE 83796

Figure 27. Test Rig Installation, D-33B Test Stand FD 36597

Preheater - The preheater assembly provided the capability of supplying vitiated combustion air to the combustor at temperatures from ambient to 1150 °F (894 °K). It was fabricated from a cylindrical housing 12 inches (30.480 cm) in diameter and contained a modified combustor from a turbojet engine. The preheater fuel nozzles were sized to give good atomization for use in an ambient pressure level rig.

Plenum Chamber - The plenum chamber functioned to provide airflow to the rig test section at uniform temperature and pressure. This was accomplished by discharging the airflow from the preheater through a multihole flow spreader into a large volume container. The plenum was fabricated from a cylinder 29.250 inches (74.295 cm) in diameter and 48 inches (121.920 cm) long. To ensure a uniform profile into the rig test section, a bellmouth flange was incorporated to transition from the plenum exit area to the test section inlet area. Bosses were installed near the exit of the plenum for the installation of temperature sensors to measure the combustor inlet temperature.

Instrumentation Section - This section housed the instrumentation used to determine the diffuser inlet total pressure, static pressure, and pressure profiles. It was designed to simulate a quarter section of the compressor discharge of a full-scale engine.

Diffuser-Combustor Case - This section housed the combustor hardware and functioned to direct the inlet airflow into the combustor liners.

Traverse Case - This section provided a platform for the combustor outlet traverse probe and actuating mechanism. The case also functioned as a rear support for the test rig.

## APPENDIX C - INSTRUMENTATION

Instrumentation was provided to measure the following parameters:

1. Combustor airflow
2. Fuel flow for each combustion zone (combustor outer and inner annuli and preheater)
3. Fuel temperature and pressure for each zone
4. Combustor inlet total temperature, total pressure and static pressure
5. Combustor outlet total temperature and pressure. The outlet static pressure was assumed to be ambient.
6. Miscellaneous diffuser and combustor total and static pressures.

A cross section of the test rig, showing the location of the various instrumentation planes, is shown in figure 28. A brief description of the instrumentation and monitoring equipment used is described below.

Airflow - As mentioned in the section on test rig hardware (Appendix B), the combustor airflow was measured with a venturi meter. The inlet total temperature and pressure sensors were located in the flow straightener approximately 12 inches (30.480 cm) upstream of the venturi throat. Two chromel-alumel, shielded thermocouples spaced 180 deg (3.141 rad) apart measured total temperature, and two kiel-type pressure probes spaced 180 deg (3.141 rad) apart measured total pressure. The static pressure at the venturi throat was measured with two wall taps spaced 180 deg (3.141 rad) apart.

The venturi inlet temperature was monitored on a 0°F to 1600°F (255.4°K to 1144.3°K) indicating potentiometer, and the total and static pressures on 0- to 80-inch (0- to 2.03-m) mercury-filled, U-type manometers.

Fuel Flow - Fuel flow to each of the three combustion zones was measured by turbine-type flowmeters. The data from these meters were monitored on a 5-channel, preset digital counter. Fuel temperature was measured by a chromel-alumel immersion thermocouple and monitored on an indicating potentiometer. Fuel pressures were measured by wall static pressure taps located in the inlet supply lines and were monitored on 0- to 1000-psig (0- to 699.6-N/cm<sup>2</sup>) pressure gages.

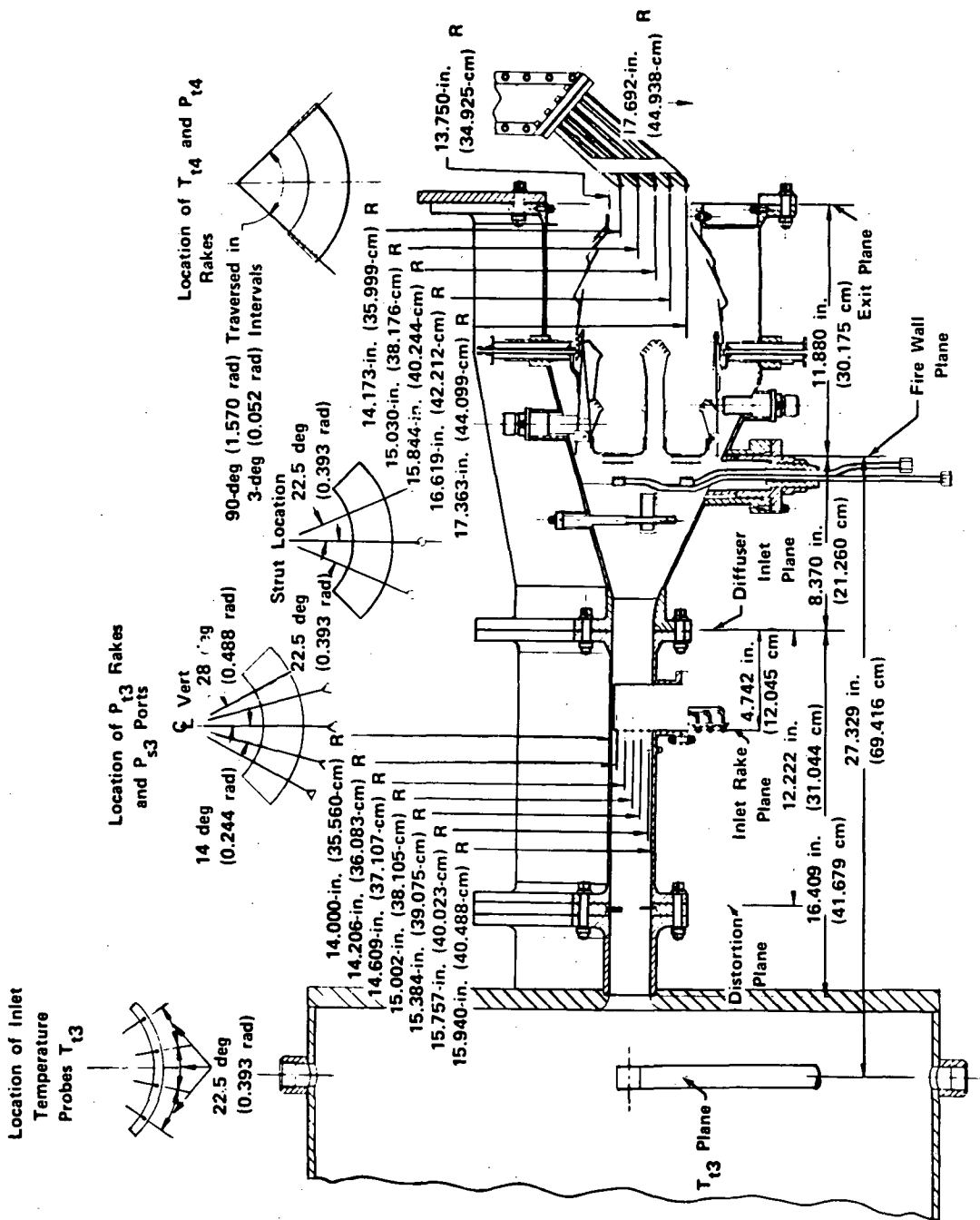


Figure 28. Test Rig Cross Section Showing Instrumentation Planes

FD 36590A

Test Section Inlet - Instrumentation to measure airflow properties at the test section inlet included:

1. Four, shielded, chromel-alumel thermocouples located as shown in figure 28. Three of these thermocouples were monitored on a 0 to 1600°F (255.4°K to 1144.3°K) indicating potentiometer. The fourth thermocouple was channeled into a temperature control unit and functioned as a preheater overtemperature abort system. The control unit was set so that if the preheater outlet temperature exceeded the desired temperature by more than 100°F (55.6°K), the test would be aborted.
2. The test section inlet total pressure was measured by five, 5-point, total pressure rakes (figure 29) located as shown in figure 28. The data from these rakes were monitored on 0- to 80-inch (0- to 2.03-m), water-filled, U-type manometers.
3. The test section inlet static pressure was measured by five wall taps located as shown in figure 28. The data from these sensors were monitored on 0- to 80-inch (0- to 2.03-m), water-filled, U-type manometers.

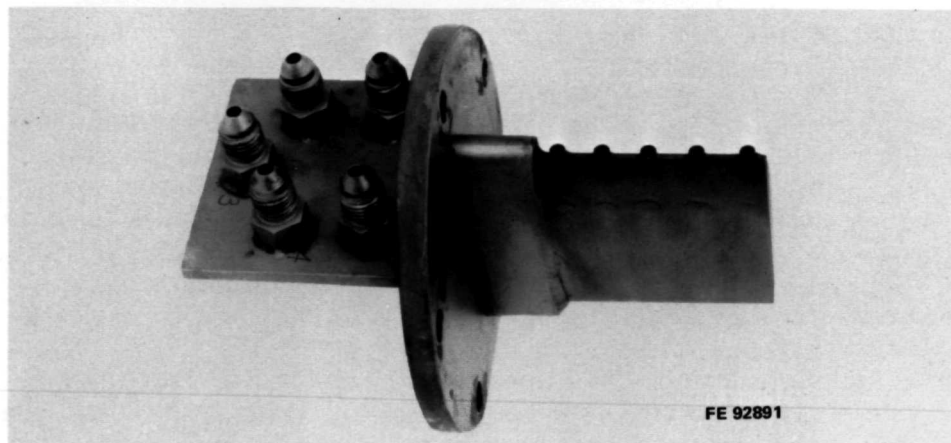


Figure 29. 5-Point Inlet Total Pressure Rake

FD 36605

Combustor Outlet - Airflow properties at the combustor outlet were measured with a 5-point total temperature and pressure rake (figure 30). Most of the temperature measurements were obtained with aspirated platinum-platinum 10% rhodium thermocouples. A high pressure steam ejector was connected across the probe exhaust to aspirate the thermocouples. The temperature data were taken in 3-deg (0.052-rad) increments across the combustor outlet and were measured on a 0°F to 3000°F (255.4°K to 1922°K) indicating potentiometer. This potentiometer was equipped with a mercury switch that would abort the test if the thermocouple being monitored exceeded 2700°F (1755°K). For a portion of the high temperature rise points the platinum-platinum 10% rhodium thermocouples were replaced with platinum-5% rhodium vs platinum-20% rhodium thermocouples. This allowed maximum local temperatures up to 3200°F (2033°K) to be set. These data were monitored as millivolt output on a 20-mv digital voltmeter.



The outlet total pressure was measured by the five 1/8-inch OD tubes shown in figure 30. These tubes were cupped on the end to increase the acceptance angle at which accurate data could be obtained. These pressure data were measured on 0- to 80-inch (0- to 2.03-m), waterfilled, U-type manometers. The outlet static pressure was assumed to be ambient.

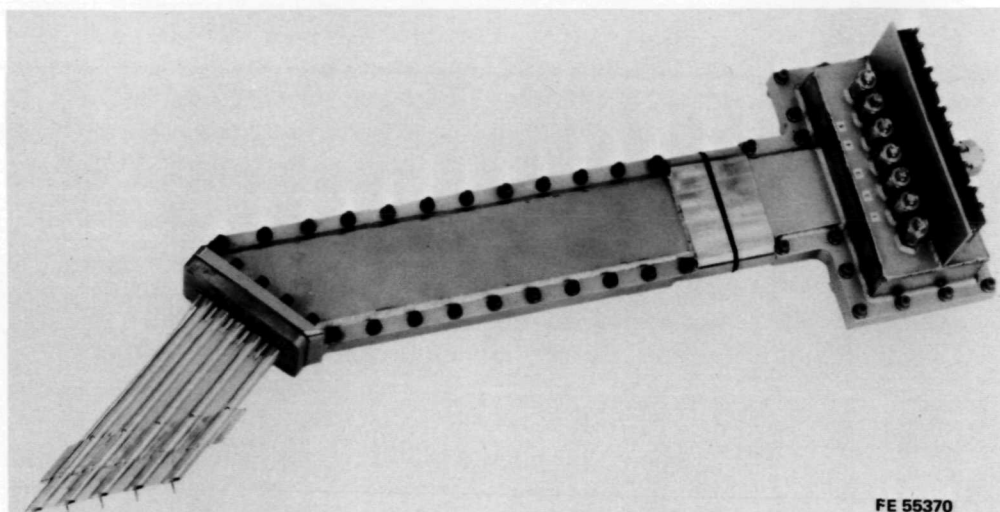


Figure 30. Outlet Total Temperature and Total Pressure Rake

FD 36604

For the maximum temperature rise tests, the platinum-rhodium rake was replaced with a 7-point iridium-iridium 40% rhodium thermocouple rake. The thermocouples on this rake were also aspirated. This rake allowed maximum local temperatures up to 3500°F (2200°K) to be realized. Although the rake was equipped with seven sensors, the outermost thermocouple failed on the initial test and was not replaced. The rake was not equipped with total pressure sensors, so pressure loss data at the maximum  $\Delta T$  points were not available.

Miscellaneous Instrumentation - Additional data channels were provided for measuring various rig pressures, such as combustor dome supply pressure, combustion zone pressures, and diffuser pressure, at various points. These data were monitored on 0- to 80-inch (0- to 2.03-m), water-filled U-tube manometers.

## REFERENCES

1. Clements, T. R. : "Interim Report - 90-Degree Sector Development of a Short Length Combustor for a Supersonic Cruise Turbofan Engine," NASA CR-72734, 1970.
2. Kitts, D. L. : "Development of a Short-Length Turbojet Combustor," NASA CR-54560, 1968.
3. Perkins, Porter J.; Schulz, Donald F.; and Wear, Jerrold D. : "Full Scale Tests of a Short-Length, Double Annular Ram Induction Turbojet Combustor for Supersonic Flight," NASA TN D-6254, 1971.
4. Chamberlain, John: "The Ram Induction Combustor Concept," presented to the AIAA Third Propulsion Joint Specialist Conference, Washington, D. C. , 18 July 1967.
5. Rusnak, J. P. and Shadowen, J. H. : "Development of an Advanced Annular Combustor," NASA CR-72453, 1969.

# DISTRIBUTION LIST FOR REPORT NO. CR-120908

1. NASA-Lewis Research Center  
21000 Brookpark Road  
Cleveland, Ohio 44135  
Attention:

Report Control Office	MS 5-5	1
Technology Utilization	MS 3-19	1
Library	MS 60-3	2
Fluid Systems Components Division	MS 5-3	1
W. L. Stewart	MS 77-2	1
J. Howard Childs	MS 60-4	1
L. Schopen	MS 77-3	1
J. B. Esgar	MS 60-4	1
H. H. Ellerbrock	MS 60-4	1
W. T. Olson	MS 3-16	1
R. R. Hibbard	MS 3-5	1
J. F. Dugan, Jr.	MS 501-2	1
Seymour Lieblein	MS 100-1	1
R. E. Jones	MS 60-6	1
Jack Grobman	MS 60-6	1
P. J. Perkins	MS 60-6	10
2. S. C. Fiorello  
Aeronautical Engine Laboratory  
Naval Air Engineering Center  
Philadelphia, Pennsylvania 19112 1
3. Aerospace Research Laboratory  
Wright-Patterson AFB, Ohio 45433  
Attention:

Dr. R. G. Dunn	1
----------------	---
4. NASA Scientific and Technical Information Facility  
P. O. Box 33  
College Park, Maryland 20740  
Attention:

NASA Representative	
RQT-2448	6
5. FAA Headquarters  
800 Independence Ave. S.W.  
Washington, D. C. 20533  
Attention:

R. W. Pinnes SS-120	
Library	1
6. NASA Headquarters  
600 Independence Ave. S.W.  
Washington, D. C. 20546  
Attention:

W. H. Roudebush	1
-----------------	---

7. Department of the Army  
U. S. Army Air Mobility Research  
and Development Laboratory  
Propulsion Division (SAUFE-PP)  
Fort Eustis, Virginia 23604  
Attention:  
    J. White 1  
    E. T. Johnson 1
8. United Aircraft of Canada, Ltd  
P. O. Box  
Longueuil, Quebec, Canada  
Attention:  
    Miss Mary Cullen 1
9. Air Force Office of Scientific Research  
1400 Wilson Boulevard  
Arlington, Virginia 22209  
Attention:  
    SREP 1
10. Defense Documentation Center (DDC)  
Cameron Station  
5010 Duke Street  
Alexandria, Virginia 22314 1
11. Department of the Navy  
Bureau of Naval Weapons  
Washington, D. C. 20025  
Attention:  
    Robert Brown, RAPP14 1
12. Department of the Navy  
Bureau of Ships  
Washington, D. C. 20360  
Attention:  
    G. L. Graves 1
13. NASA-Langley Research Center  
Langley Station  
Technical Library  
Hampton, Virginia 23365  
Attention:  
    Mark R. Nichols 1  
    John V. Becker 1
14. United States Air Force  
Aero Propulsion Laboratory  
Area B, Bldg. 18D  
Wright-Patterson A. F. B., Ohio 45433  
Attention:  
    Robert E. Henderson 1

15. United Aircraft Corporation  
Pratt & Whitney Aircraft Division  
400 Main Street  
East Hartford, Connecticut 06108  
Attention:
  - G. Andreini 1
  - Library 1
  - R. Marshall 1
  
16. United Aircraft Research  
East Hartford, Connecticut  
Attention:
  - Library 1
  
17. Allison Division of GMC  
Department 8894, Plant 8  
P. O. Box 894  
Indianapolis, Indiana 46206  
Attention:
  - J. N. Barney 1
  - G. E. Holbrook 1
  - Library 1
  
18. Northern Research and Engineering Corp.  
219 Vassar Street  
Cambridge, Massachusetts 02139  
Attention:
  - K. Ginwala 1
  
19. General Electric Company  
Flight Propulsion Division  
Cincinnati, Ohio 45215  
Attention:
  - Technical Information Center N-32
  - D. Bahr 1
  
20. General Electric Company  
1000 Western Avenue  
West Lynn, Massachusetts 01905  
Attention:
  - Dr. C. W. Smith 1
  - Library Building 2-40M 4
  
21. Curtiss-Wright Corporation  
Wright Aeronautical Division  
Woodridge, New Jersey 07075  
Attention:
  - D. Wagner 1
  - W. Walker 1

22. AiResearch Manufacturing Company  
402 South 36th Street  
Phoenix, Arizona 85034  
Attention:  
Robert O. Bullock 1
  
23. AiResearch Manufacturing Company  
9851 Sepulveda Boulevard  
Los Angeles, California 90009  
Attention:  
Dr. N. Van Le 1
  
24. AVCO Corporation  
Lycoming Division  
550 South Main Street  
Stratford, Connecticut 06497  
Attention:  
Claus W. Bolton 1  
Charles Kuintzle 1
  
25. Continental Aviation and Engineering Corporation  
12700 Kercheval  
Detroit, Michigan 48215  
Attention:  
Eli H. Bernstein 1  
Howard C. Walch 1
  
26. International Harvester Company  
Solar Division  
2200 Pacific Highway  
San Diego, California 92112  
Attention:  
P. A. Pitt 1  
Mrs. L. Walper 1
  
27. Goodyear Atomic Corporation  
Box 628  
Piketon, Ohio  
Attention:  
C. O. Langebrake 1
  
28. George Derderian AIR 53622 B  
Department of the Navy  
Bureau of Navy  
Washington, D. C. 20360 1
  
29. The Boeing Company  
Commercial Airplane Division  
P. O. Box 3991  
Seattle, Washington 98124  
Attention:  
G. J. Schott MS 80-66 1

30. The Boeing Company  
Missile and Information Systems Division  
224 N. Wilkinson Street  
Dayton, Ohio 45402  
Attention:  
Warren K. Thorson 1
31. Aerojet-General Corporation  
Sacramento, California 95809  
Attention:  
M. S. Nylin 1  
Library 1
32. Cornell Aeronautical Laboratory  
4455 Genessee Street  
Buffalo, New York 1
33. Marquardt Corporation  
16555 Saticoy Street  
Van Nuys, California 1
34. Thompson Ramo Wooldridge  
23555 Euclid Avenue  
Cleveland, Ohio 1
35. Aro, Incorporated  
Arnold Air Force Station  
Tennessee 1